ADAMA SCIENCE AND TECHNOLOGY UNIVERSITY

SCHOOL OF ELECTRICAL ENGINEERING AND COMPUTING

ELECTRICAL AND COMPUTER ENGINEERING DEPARTMENT

Investigation of Efficient Antenna Array Polarization and Beamforming for the Cognitive Radio Application

By
Niguse Borsamo

A Thesis Submitted to the Department of Electrical and Computer Engineering, School of Electrical Engineering and Computing, Adama Science and Technology University in meeting the Preliminary Thesis Requirement for the Award of Degree of Master of Science in Communication Systems Engineering

MAY 2018

ADAMA, ETHIOPIA

ADAMA SCIENCE AND TECHNOLOGY UNIVERSITY

SCHOOL OF ELECTRICAL ENGINEERING AND COMPUTING

ELECTRICAL AND COMPUTER ENGINEERING DEPARTMENT

Investigation of Efficient Antenna Array Polarization and Beamforming for the Cognitive Radio Application

By

Niguse Borsamo

Approval by Board of Examiners

__________________________________ __________

Chairman, Dept. Graduate Committee Signature

DR. Feyisa Debo __________

Advisor Signature

__________________________________ __________

Internal Examiner Signature

__________________________________ __________

External Examiner Signature

Declaration

I, the undersigned, declare that this thesis is my original work has not been presented for a degree in this or any other university, and all sources of materials used for the thesis have been fully acknowledged.

Niguse Borsamo ____________

Name Signature

This thesis has been submitted for examination with my approval as a university advisor.

DR. Feyisa Debo ____________

Advisor's Name Signature

Date of Submission: ______________________

Acknowledgement

I would like to take this opportunity to express my sincere gratitude and many thanks to the people who have made completion of this thesis possible. This is a difficult task since words alone cannot express how grateful I am to all of them.

First and foremost, I would like to express my sincere thanks to my adviser Dr. Feyisa Debo his excellent advise and continuous support during the work of this thesis. Without his guidance and encouragement several breakthroughs in this thesis would be impossible to be achieved.

I would also like to express my gratitude to staff members and students at the electrical and computer engineering department, Adama Science and Technology, for their friendship and help by any means during my years at the university.

Besides them, I am especially indebted to my parents for their love, sacrifice and support. They are my teachers after I came to this world and have set great example for me about how to live, study and work.

At last, I would like to give thanks to God since He has given me wisdom, health and all the necessities that I need for all these years.

Abstract

Radio spectrum is becoming increasingly scarce as more and more devices go wireless. Meanwhile, studies indicate that the assigned spectrum is not fully utilized. Cognitive radio (CR) technology is envisioned to be a promising solution to address the imbalance between spectrum scarcity and spectrum underutilization. It improves the spectrum utilization by opportunistically accessing the unused or underutilized spectrum owned by primary systems. However, because of spectrum sharing, the interference problem is always the limiting factor that hinders the practical implementation of CR network. In this thesis, we focus on mitigation of interference problems in the uplink of CR BS system by exploiting signal processing in combined polarization ad spatial domain. In fact, the main objective of this work is to study and recommend optimal antenna array polarization and robust adaptive beamforming algorithms for uplink of CR-Base Station (CR-BS) which can reduce the effects of interference, noise, and multipath fading.

We have proposed to equip a CR-BS receiver system with dual-polarized array of crossed-dipole antenna. In the beamformer design, we studied and investigated three adaptive algorithms namely; Quaternion-valued Minimum Variance Distortionless Response (QMVDR), Quaternion-valued worst case constraint (QWCC), and Quaternion-valued Least Mean Square (QLMS) beamformers. The mathematical analyses of these algorithms are carried-out, and performance surfaces such as; output Signal-to-Interference plus Noise Ratio (SINR), beampatterns, and mean square error are investigated. Matlab simulation test-bed is created to compare the performance of these three robust algorithms with those of conventional adaptive beamforming algorithms presented in literature. It is shown from the simulation results that all the proposed algorithms can outperform the other algorithms in all the test conditions (e.g., identical and separate polarization states of desired signal and interference, small and large angle separation, etc.).

Finally from analysis and simulation results it is proved that a CR BS system employed with dual-polarized antenna array and adaptive algorithm at uplink can adaptively enhance the signals of CR users by matching in polarization as well as Direction of Arrival (DOA). Furthermore, the interference mitigation becomes more effective due to the possibility of filtering in both polarization and DOA, thereby enabling spectrum sharing for CR even in severe interference scenario.

Table of Contents

List of Figures

List of Tables

Abbreviations

CR……………………………………………………………………………Cognitive Radio

DOA………………………………………………...…………………Direction of Arrival

PUs…………………………………………………………………………..Primary Users

SUs……………………………………………………………………….Secondary Users

ITU……………………………………………………International Telecommunication Union

CR-BS…………………………………………………………Cognitive Radio-Base Station

SDMA……………………………………………………...Spatial Division Multiple Access

PDMA…………………………………………………...Polarization Division Multiple Access

SINR……………………………………………………Signal-to-Interference plus Noise Ration

SNR…………………………………………………………………Signal-to-Noise Ratio

QoS………………………………………………………………………...Quality of Service

EM………………………………………………………………………...Electromagnetic

LCMV……………………………………………………...Liner Constrained Minimum Variance

MVDR…………………………………………Minimum Variance Distortionless Response

LMS…………………………………………………………………...Least Mean Squares

SMI………………………………………………………………Sample Matrix Inversion

CMA…………………………………………………………Constant Modula Algorithm

RLS………………………………………………………………Recursive Least Squares

AWGN……………………………...………………… Additive White Gaussian Noise

NS…………………………………………………………………………………Null Steering

MSE……………………………………………………………………...Mean Squared Error

MNV…………………………………………………………....Minimum Noise Variance

IC…………………………………………………………………………...Interference Cancellation

ESPRIT…………………..….Estimation of Signal Parameters via Rotational Invariance Techniques

ML………………………………………………………………………… Maximum Likelihood

DSA…………………………………………………………………Dynamic Spectrum Access

FCC………………………………………………………Federal Communication Commission

MAC………………………………………………………………………...Medium Access Control

ULA………………………………………………………………………....Uniform Linear Array

TEM………………………………………………………………..Transverse Electromagnetic

QMVDR……………….……….....Quaternion-valued Minimum Variance Distortionless Response

QWCC………………………………….…….………Quaternion-valued Worst Case Constrained

QLMS…………………………………….……………Quaternion-valued Least Mean Squares

CHAPTER ONE

INTRODUCTION

1.1 Background and Motivation

Many appealing applications of wireless communications have been emerging, such as mobile internet access, health care, medical monitoring and smart homes. There has also been a remarkable growth in designing and manufacturing various smart sensors, including for health care, transportation, environment monitoring and so on with an increasing demand of versatile wireless services. Another emerging trend of current wireless services is the demand of high data rate wideband services.

Due to the above ever growing demand for wireless services by the customers there has been heavy demand and occupancy of frequency spectrum between 1-6 GHz. This problem has placed a heavy burden to the resource allocation policy maker to accommodate between the demand and the available spectrum resources. However, according to the snapshot of spectrum usage in the urban area shown in Figure 1-1 provided from the recent studies, we can see that there is actually very little usage on the licensed spectrum especially on the spectrum between 3-6 GHz. This fact is contradicting with the mindset of spectrum scarcity, since we can see that there is spectrum abundance.

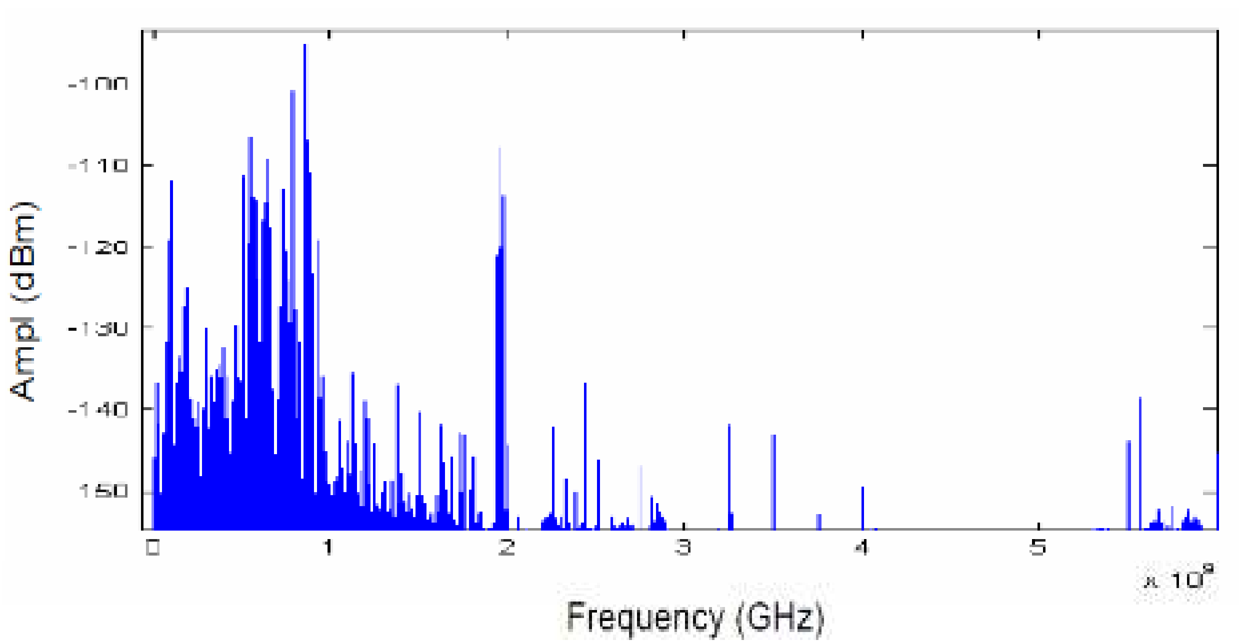

Figure 1.1 Snapshot of spectrum utilization until 6 GHz in urban area [1]

The low level of spectrum usage also contradicts with the resource allocation policy maker. The spectrum allocation chart of Federal Communication Committee (FCC) in Figure 1.2 shows multiple allocations over the frequency bands and “exclusive rights” policy that states if a licensed system is not transmitting, its spectrum remains off-limits to other users. This contradiction shows that the spectrum scarcity is a product of the regulatory and licensing process by the authority and this condition indicates that a new approach to the spectrum licensing is needed.

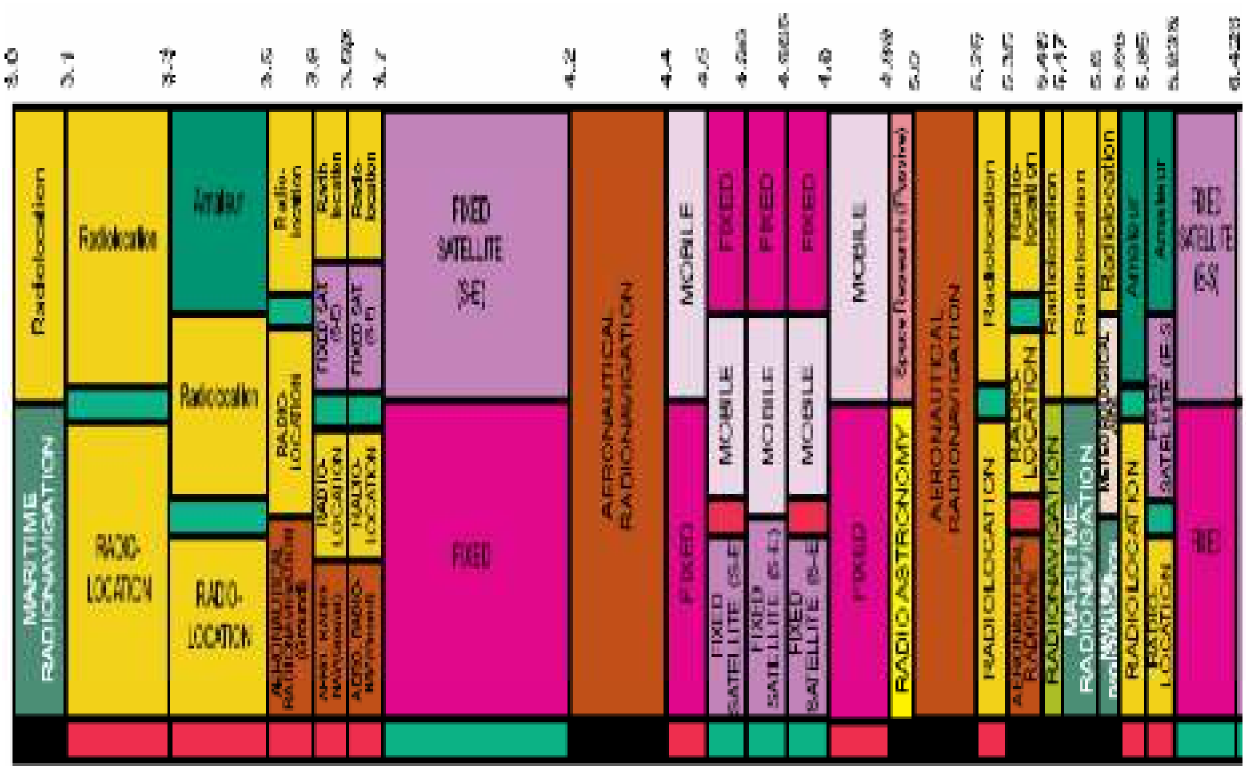

Figure 1-2 Frequency allocations charts of FCC from 3-6 GHz [2].

Thus, policy makers have been considering more comprehensive and flexible uses of the available frequency spectrum. Hence there is a need to develop an energy efficient green technique which is capable of optimizing the usage of spectrum. An approach which is innovated to solve the problem of spectrum scarcity is Cognitive Radio (CR) system. CR has been initially introduced by Dr. Joseph Mitola, and it is developed to be able to sense the spectral environment over the available band and to use the unused spectrum as long as it doesn’t interfere with the licensed users called Primary Users (PUs) [3].

The CR provides three various solutions to accommodate under-utilized spectrum for use by unlicensed wireless devices. They *"underlay", "overlay"* and *"interweave"* its signals with those of the PUs in such a way that the communications by PUs is as unaffected as possible [4]. The underlay approach protects PUs by enforcing a spectral mask on CR signals so that the interference generated by CR devices is below the acceptable noise power at the PUs. The overlay approach also allows concurrent PUs and CR transmissions, but the enabling premises for the overlay system are that the CR users can use part of their power for secondary communication and the remainder of the power to assist (relay) primary transmissions. Based on the idea of opportunistic communication, J. Mitola proposed the interweave approach. Being able to have dynamic access to the spectrum, CR must detect the existing temporary frequency voids, referred to as spectrum holes that are not in use by PUs, and then be technically able to autonomously resolve conflicts in spectrum access by avoiding interference with incumbent signals.

There are several domains to achieve the spectrum sharing with CR such as; time, frequency, space, and region [5]. In time users can share spectrum as when taxicabs alternately use the same frequencies or citizen band radio operators share frequencies. By detecting spectrum holes and making use of the temporally unoccupied spectrum bands, CR in frequency domain can have efficient utilization of the spectrum via employing the interweave spectrum access mode. In space domain, if CR is able to transmit signals to its users while ensuring those signals are unable to be received by PUs or at PUs the received power of CR signals is below the interference constraint level of PUs, CR is able to adopt the underlay spectrum access mode of utilizing the spectrum. Due to the advancements in antenna array technology, antenna polarization dimension may also be exploited as an additional degree of freedom for spectrum sharing. These are the promising available domains, where the CR system is used by the SUs to access the spectrum of the PUs.

In CR terminology the PUs has the priority and legality to access the communication spectrum, and the CR users are allowed to use the spectrum only if they do not create harmful interference to the primary network users. Interference is one of the key factors affecting the wireless network performance and has been a long-lasting problem coupling wireless communication system. In the context of CR networks, the interference issues are extremely important. Its paramount significance lies on two aspects. On one hand, CR holds the fundamental premise of not causing any detrimental interference to the primary system. On the other, the CR network performance may be limited by interference coming from either the primary or undesired SUs transmission. In addition to this since SUs are required to minimize their transmission power in order to meet PUs interference constraint, at the uplink of CR-Base Station (CR-BS) it's difficult to detect the SUs signal which is corrupted by interference, noise, and multipath channel effects. Therefore, the CR system needs some techniques in its architecture to adapt its radio parameters in order to address the aforementioned problems. To this end, this thesis work studies the Interference Cancellation (IC) techniques in the uplink of CR-BS.

Modern antenna array technology in conjunction with beamforming as spatial filtering offers a promising solution to minimize co-channel interference, noise and multipath channel effects [6, 7]. This technique has been first introduced into Radar and Sonar systems when the desired signal and interferences occupy the same temporal frequency band and thus temporal filtering cannot be applied to separate desired signals from interferences. It utilizes the spatial diversity taking into account that the desired and interfering signals usually originate from different directions. This therefore allows for an approach which spatially separates desired signals from interferences. By using antenna arrays with adaptive beamforming in a CR system, it is possible to reduce the amount of co-channel interference, noise and multipath channel effects and further increase the system capacity.

So far, there has been a great deal of research on the ability of adaptive space antennas to cancel interference in wireless systems [6-9], but a little has been done on the advantages of polarization domain, which can create polarization canceller [11-14]. If a wireless receiver detects and exploits more than one polarization state of the signal by the help of diversely polarized antenna, it can match the polarization of a desired signal and/or null an interferer having the same direction of arrival, when the two signals have different polarization states. For example if wireless base stations or nodes in a peer-to-peer system can match the polarization states of hand-held transceivers, link quality and reliability will be enhanced. Diversely polarized antenna has also the potential of overcoming multipath channel effects in which detected multipath components can be combined by some proper combining techniques to enhance Signal-to-Interference plus Noise Ratio (SINR) [10]. Further diversely polarized antenna has the capability to support multi polarization states of planar waves, which can allow several distinct information channels. Thus the advantage of doubling total number of available degree of freedom for spectrum sharing can be achieved in CR network [11].

The dual antenna polarization cancellers operate purely in the polarization domain, while adaptive beamformers based on uniformly polarized array elements operate only in the spatial (angle domain). It is also possible to combine these two domains in a single algorithm by applying signal processing techniques to an antenna array with multi-polarization elements. Using such an algorithm can really create an opportunity to distinguish desired signal from interferers on basis of polarization as well as Direction of Arrival (DOA). It is possible that 100 percent or greater increase in system capacity can be achieved through combination of spatial- and polarization-division multiple access (SDMA/PDMA). A combined spatial-and-polarization signal processing is recently used in mobile base station systems to provide interference mitigation and enhance user capacity, data rates [12]. [13] Current applications of multi-polarized antenna array based beamforming are predominately in radar detection, sonar, and seismic due to area and processing power requirement.

1.2 Statement of the Problem

Although the CR system has been proposed as a potential solution to optimize spectrum utilization its Quality of Service (QoS) is inevitably affected by interference coming from PUs and undesired SUs transmission. Hence, interference protection is essential to the coexistence of PUs and CR systems. In the previous works several interference mitigation techniques have been studied in the CR-BS receiver architecture [14-16]. One of those techniques is beamforming as spatial filtering. Beamforming techniques exploit DOA difference to separate desired signal from interference. Several optimum and adaptive beamforming algorithms such as, Liner Constrained Minimum Variance (LCMV), Minimum Variance Distortionless Response (MVDR), Least Mean Squares (LMS), Sample Matrix Inversion (SMI), Constant Modula Algorithm (CMA) Recursive Least Squares (RLS), and the likes, were developed, studied and proposed for the uplink of CR-BS system [17-20]. Performance measurement criteria such as Output SINR, strength of beampattern, sidelobe levels, and speed of convergence are analyzed for those algorithms and suggestions are made that which one is best according to CR-BS system application.

Most of the previous works on beamforming are derived by the use of scalar antenna arrays, and it is noticed that scalar arrays can only provide single component of amplitude information from the vector electromagnetic signal. However at the uplink of CR-BS it is difficult to obtain accurate information of the CR user signal from the single component of electromagnetic wave. In addition to this, they assume that the polarizations of the receiving antenna array and impinging signals are perfectly matched. But, in practical sense the signal polarization may be altered by some factors and the resulting polarization mismatch will affect the array detection performance. Further beamforming technique by nature fails to separate desired signals from interference in case of small DOA separation and its performance degrades substantially, when uncertainty of DOA exists. Finally beamforming techniques in the context of CR-BS architecture have been not well studied.

How can we detect and exploit two orthogonal components of the electromagnetic signal and improve system performance? Does it possible to match signal polarization in order to mitigate polarization mismatch loss, and further improve link quality at CR-BS? Does it possible to distinguish or mitigate interferences on basis of polarization in addition to DOA? And, also which antenna array polarization and signal processing algorithms perform well for the uplink of CR-BS system? Such types of investigations are very important for CR system designer to select optimal antenna array polarization and algorithms depending on the required conditions.

This thesis work first discusses the feasibility of the proposed technique to this intelligence system. Then after survey of various antenna arrays and adaptive algorithms are carried-out and, performance evaluation based on certain defined criteria is performed. Finally the thesis suggests robust algorithms and suitable array type to CR-BS receiver architecture.

1.3 Objective of the Study

1.3.1 General Objective

The main aim of this thesis work is to investigate efficient antenna array with adaptive polarization-space signal processing algorithms for use in the uplink of a CR-BS system, and performance evaluation of investigated algorithms with that of the algorithms presented in the literature.

1.3.2 Specific Objectives

Specifically the aim of this thesis is to:

- To study on the possibility of antenna polarization dimension and beamforming techniques as interference mitigation methods in a CR system.
- Performance evaluation of scalar antenna array and electromagnetic vector antenna array based on array detection capability, computational complexity, and cost of implementation.
- Performance evaluation of existing scalar array based adaptive beamformers such as; LMS, SMI, RLS, CMA, and their limitation under certain condition.
- To study the effect of varying signal polarization and direction of arrival (DOA) on adaptive array beamforming performance criteria's such as; the main beam direction, side-lobe levels and placing of nulls in the direction of interferers.
- To investigate the performances of different robust polarization-space adaptive beamforming algorithms such as Quaternion-valued minimum variance distortionless response (QMVDR), Quaternion-valued worst case constraint (QWCC) and Quaternion-valued least mean square (QLMS) based on proposed dual polarized antenna array.
- Recommendation of best algorithm and antenna array type which can be deployed for CR-BS receiver architecture.

1.4 Scope of the Study

This thesis investigates optimal antenna array polarization and adaptive beamforming algorithms for CR system application. This work tries to evaluate the performance improvement that can be achieved at the uplink of CR-BS, when signal processing in combined polarization-and-space is exploited. Note that this work only considers a scenario of the CR-BS receiver that is usually found in uplink channels in CR communications.

This is done by developing the appropriate system model of idealized wireless communication environment (transmitter, channel type, receiver) and defining the necessary signal and array parameters. Firstly proposed array geometries with necessary parameters are developed and those geometries ability to effectively receive electromagnetic signals using an assortment of different algorithms are tested. Secondly, after the design of appropriate antenna array geometries, signal environments of the CR user and interferers are defined. The additive white Gaussian (AWGN) channel model is deployed to the signal model. Thirdly, M-file codes are written in Matlab for the three proposed algorithms. Finally designed communication system model is simulated through Matlab 2017a software with appropriate simulation tool. From simulation results performance evaluations are performed interms of certain defined criteria.

1.5 Review of Related Works

So far a number of research papers have been published regarding on spectrum sharing using interweave, underlay, and overlay schemes in CR [4]. In CR network SUs opportunistically utilize spectral holes of licensed band in space, time, frequency or possibly using polarization domain which are not occupied by the PUs. However, because of the spectrum sharing nature in CR network the communication systems operates with intensive interferences. Therefore it is necessary to apply IC techniques in CR architecture in order to guarantee reliable communication.

A few interference mitigation techniques have been studied in the context of CR system architecture [14]. The authors in those works have presented an opportunistic mitigation scheme for CR-BS receivers to adaptively cancel the PUs signals when they are unable to decode these signals. Many other interference mitigation techniques can be found in [15, 16]. They have used a filter based approach, transform-domain approach, cyclostationary based approach, higher-order statistics-based approach, and spatial processing also referred to as beamforming technique. Almost all interference mitigation techniques are proposed and discussed based on studies of CR transmission and reception in the signal domain, transform domain, frequency domain, waveform domain, antenna system characteristics and space domain. Our work focuses on exploiting joint space-polarization domain to CR receiver architecture.

In the recent works numerous fixed algorithms have been developed, studied, and proposed for the application in CR technology. In [17], [18] traditional fixed beamforming algorithms such as: LCMV, MVDR, and Null Steering (NS) beamformers were proposed, which has a drawback of system performance and lack of adaptive techniques. Hence, this thesis proved that in case of DOA uncertainty, they are not robust to steer the main beam to specific desired direction and place deep nulls in the direction of interferer. Therefore, the beamforming problem has been reformulated to assign the weighting values based on the statistics of the received data vectors.

One approach of alleviating these problems is the use of spatial processing with adaptive algorithms which assign the weight coefficients based on statistics of the data. Recent developments in adaptive beamformers [19, 20] have resulted into the LMS, SMI, RLS, CMA, and Least Square-Constant Module (LS-CMA). These adaptive algorithms are analyzed based on computational complexity, cost of implementation, and performance criteria's such as; SINR, average beampattern level, side lobe levels, and Mean Squared Error (MSE) levels. Simulation results show that LMS has low speed of convergence, successfully steer the main lobe of radiation pattern towards the desired direction, but unsatisfactory to nullify the interference compared to the other algorithms. The other adaptive algorithms have fast speed of convergence and forming deep nulls but high computational cost, complexity of analysis. These adaptive algorithms relatively can combat DOA uncertainties, but they are often conservative and only suitable in case of small DOA errors and large angle separation.

In [21, 22] adaptive beamformers from both blind and non-blind iterative algorithms that suit the CR technology were further studied considering similar performance criteria. The study has shown that an SMI from the non-blind beamforming family and CMA from blind beamforming family have better performance levels. The others have low and dying side lobes. The paper revealed that, when overall performance is considered, the SMI is preferred for CR applications as compared to the other adaptive beamforming algorithms. Almost all beamforming algorithms developed and studied on [17-22] are derived based on the use of scalar antenna arrays which exploit only DOA, and didn't consider polarization property of the signal. However the performance of beamformers may degrade substantially due to polarization mismatch of the impinging signals.

In [10, 11] it has been shown that the performance of array signal processing can be significantly enhanced when polarization information of the signal is exploited in addition to DOA. The use of combined polarization-space adaptive beamforming algorithm based on sensor arrays of different polarization with co-located elements has been initially considered as a means of rejecting jammers in military applications [23]. After that it has been studied in radar receivers where the polarmetric diversity is used to improve the estimation, detection, and tracking of the target [24]. Furthermore the potential of joint polarization-space filtering for interference rejection in cellular BS systems has been investigated in recent years [12], and [25]. On those works it was indicated that 20 to 35 dB of interference rejection is possible if interfering and desired signals differ in either polarization state or angle DOA. However, neither measurements nor simulations have been reported showing the performance of a combined polarization-space adaptive signal processing algorithm as IC in a CR-BS receiver system.

The so-called crossed-dipole and tripole were first introduced into the field of adaptive arrays in [26, 27]. Based on such a system, the complex-valued adaptive beamforming problem was studied in detail in terms of the output SINR [27]. To enhance its robustness, many methods have been proposed, such as diagonal loading [28-31], and those based on the optimization of worst-case performance [32-34].

Very recently, improved robustness against steering vector mismatch errors has been shown by quaternion formulations [35-38]. The quaternionic version of the conventional MVDR Beamformer has been derived with a two component EM vector-sensor array in [35, 36], where a better performance is obtained in the presence of steering vector mismatch errors. Afterwards, based on the idea of two-way interference and noise cancellation (INC) a quaternionic adaptive beamforming scheme was presented by adopting a combined structure to achieve an improved performance in the context of one strong coherent interference [37, 38]. However, neither study nor measurement has been reported that show the performance and possible deployment of these techniques in CR-BS system applications.

During the past few decades, many subspace-based techniques have been adapted to diversely polarized arrays to estimate DOA and polarization of the narrowband electromagnetic sources [39, 40]. The Estimation of Signal Parameters via Rotational Invariance techniques was used for two-dimensional angle and polarization estimation [39]. A novel algorithm to estimate the DOA and polarization of a completely polarized polynomial-phase signal of an arbitrary degree with dual polarized vector-sensor was proposed in [40]. The algorithm can estimate DOA and polarization parameter without a priori knowledge of the polynomial-phase signal's coefficients and the signal's frequency spectrum. The maximum likelihood (ML) and MVDR estimators for DOA and polarization parameters were derived in a multipath environment.

Basically, this works mainly focuses on investigation of efficient antenna array polarization and robust spatiotemporal-polarization signal processing algorithms to CR-BS receiver. Performance of different algorithms with specified array configuration is compared under the conditions of uncertainty of DOA, different polarization state, and spatial separation variation based on certain performance measurement criteria. Such types of issues need to be analyzed more to recommend an algorithm and array parameters which is best, under a given performance criterion.

1.6 Methodology

The methods to be employed to achieve the objectives of the research are:

- **Literature Review:** includes reading books, articles, simulation tools and other resources related to the topic, that can help to understand the nature of the problem that need to be solved and its importance, also reviewing the important aspects related to the topic.
- **System Modeling:** involves the structure of the system to be simulated along with the formulation of algorithm that is used in this thesis (such as mathematical and logical modeling). Also defining the appropriate procedures to be deployed for implementing the adaptive algorithm, and organizing it in a flow chart if necessary to facilitate the simulation step.
- **Simulation:** involves simulating the modeled communication system for proposed algorithms with corresponding antenna array by Matlab and appropriate simulation tools. Math-works MATLAB R2017a is used throughout to write and run M-files that implement various algorithms.
- **Analysis and Interpretation of the results:** the results obtained from simulation are analyzed and compared based on performance analysis criteria. Therefore the research finding can be clearly stated, thus based on it the conclusion is derived.

1.7 Contribution of Thesis Work

This thesis work first carry out a comprehensive review on a variety of interference mitigation techniques applicable to uplink of CR-BS. Then it focus on combined polarization-and-spatial signal processing for CR-BS receiver systems to mitigate interference occurrences from primary network users and undesired SUs in order to improve receiver performance. Since array detection performance will be altered by polarization mismatch, optimal polarization array selection is of particular interest. Then three quaternion-valued adaptive QMVDR, QWCC, and QLMS beamforming algorithms are investigated based on the proposed two-component sensor arrays for uplink application of CR-BS. The results of three adaptive algorithms are compared in several scenarios such as various DOA and polarization separation, and input SNR. The effect of signal polarization information and DOA separation on beamformers performance is studied. After the comparison, we can then decide which beamforming algorithm gives better performance among the presented methods.

CHAPTER TWO
OVERVIEW OF COGNITIVE RADIOS

2.1 INTRODUCTION

During the last few decades, the severe shortage of radio spectrum has been the main motivation always used by researchers in the field of wireless communications. It has been believed that this shortage is mainly due to the physical scarcity of radio spectrum and the rapid spread of diverse devices with wireless-interaction capability, such as mobile phones, laptop computers, home appliances, wireless tags, etc. Traditional and common approaches to solve this problem have been to increase the number of bits that can be transmitted per unit time and frequency, resulting in high capacity within a given frequency bandwidth. To this end, considerable research effort and fund have been spent to develop those methods.

However it has been stated from the recent studies, the scarcity of frequency spectrum is not due to physical scarcity rather than the static assignment of the spectrum which results in inefficient usage of the spectrum. The utilization of the spectrum can be as low as 10% in some geographical location and time. Thus policy makers need Dynamic Spectrum Access (DSA) schemes which can be considered as a method for solving spectrum scarcity. In this context, CR communication has emerged as a promising solution to address the spectrum scarcity problem by exploring spectral opportunities in the primary licensed spectrum in several domains such as, frequency, time, or space, thus facilitating the secondary unlicensed spectrum access [5]. This can considerably improve the spectrum utilization.

However, since CR operates in the same spectrum band with licensed or primary network, its communication is affected by the primary transmission. To alleviate these challenges of CR techniques, several techniques have been considered in CR architecture; such as wave shaping, transmission power control, beamforming, antenna system characteristics, and etc. [14-16]. In this introductionary chapter, we first introduce definition of CR, several existing concepts of CR, revealing CR intelligence and the capabilities of spectrum estimation and adaptation.

2.2 Concepts of the CR

Though the concept of CR has been introduced, and the prototypes, applications and essential components of CR have been developed, the CR community has by far not agreed upon exactly what is and is not CR. However, some of the prominent offered definitions of CR are the following:

Joseph Mitola defines CR as "A radio that employs model-based reasoning to achieve a specific level of competence in radio-related domain" [3].

[41] Simon Haykin defines CR as "An intelligent wireless communication system that is aware of its surrounding environment (i.e., outside world), and uses the methodology of understanding-by-building to learn from the environment and adapt its internal states to statistical variations in the incoming RF stimuli by making corresponding changes in certain operating parameters (e.g., transmit-power, carrier-frequency, signal polarization, and modulation strategy) in real-time, with two primary objectives in mind:

- Highly reliable communications whenever and wherever needed
- Efficient utilization of the radio spectrum

Coming from a background where regulations focus on the operation of transmitters, FCC has defined CR as "A radio that can change its transmitter parameters based on interaction with the environment in which it operates" [42].

While aiding the FCC in its efforts to define CR, IEEE USA offered the following definition [43]: "A radio frequency transmitter/receiver that is designed to intelligently detect whether a particular segment of the radio spectrum is currently in use, and to jump into (or out if necessary) the temporarily-unused spectrum very rapidly, without interfering with the transmissions of other authorized users."

The broader IEEE tasked the IEEE 1900.1 group to design CR which has the following working definition: "A type of radio that can sense and autonomously reason about its environment and adapt accordingly. This radio could employ knowledge representation, automated reasoning and machine learning mechanisms in establishing, conducting, or terminating communication or networking functions with other radios. CR can be trained to dynamically and autonomously adjust its operating parameters." [44, 45]

Though, there exists no universal agreed CR definition, the above definitions reveal some commonalities, such as adaptation and autonomous environment sensing abilities. In general, CR is capable of acquiring information about its operating environment. Additionally, it is capable of changing its waveform and applying information, which implies that CR has intelligent adaptations.

2.3 Spectrum Sharing Schemes in CR

The condition of the licensed electromagnetic spectrum can be described as,

- ❖ Some frequency bands in the spectrum are largely unoccupied most of the time.
- ❖ Some of the frequency bands are partially occupied.
- ❖ The remaining frequency bands are heavily occupied.

Thus, SUs can access the primary licensed spectrum opportunistically by exploiting spectral holes/white spaces in time, frequency, and space as in Figure 2.1, or allowed to operate in the same spectrum band as long as the secondary transmissions guarantee the protection of the primary receivers.

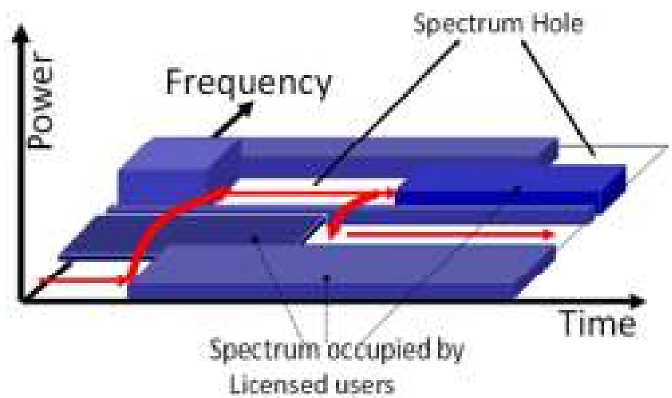

Figure 2.1 Illustration of spectrum white space [46].

Based on the access technology employed by the secondary system, the available spectrum exploitation paradigms can be categorized into: (i) interweave, (ii) underlay and (iii) overlay [5, 43]. The underlay approach allows concurrent primary and secondary transmissions in a manner as used in Ultra wideband (UWB) systems. Underlay systems protect PUs by enforcing a spectral mask on the secondary signals so that the interference generated by the secondary devices is below the acceptable noise floor of the spectrum used by the PUs of the spectrum. The spectral mask constraints are compensated by access to a wide bandwidth over which the secondary signal can be spread and dispread in order to provide sufficient signal-to-noise (SNR) for secondary communications. However, the interference power constraints associated with underlay systems allow short-range communications only.

The overlay approach also allows concurrent primary and secondary transmissions. The premises for an overlay system are that the secondary users can use part of their power for secondary communication and the remainder of the power to assist (via relay) the primary transmissions. By careful choice of the power split, the increase in the PUs' SNR due to the assistance from secondary relaying is compensating for the decrease in the PUs' SNR due to interference caused by the remainder of the secondary transmit power that is used for secondary communication.

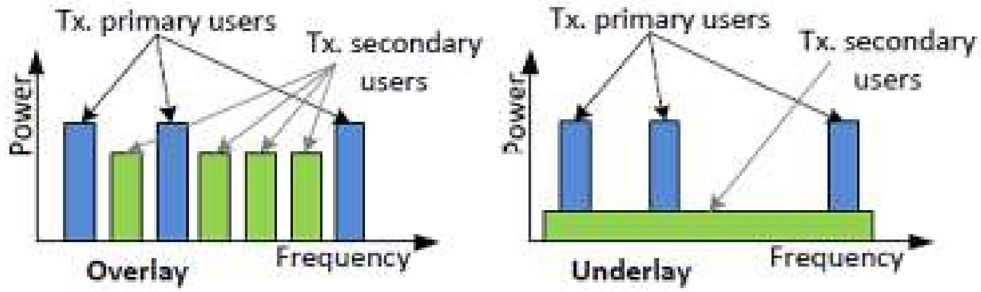

Figure 2.2 Spectrum sharing schemes for CR [5]

Based on the idea of opportunistic communication [3], J. Mitola proposed the interwave approach. Recent studies conducted by the FCC and industry show that a major part of the spectrum is not utilized most of the time. In other words, there exist temporary frequency voids, referred to as spectrum holes that are not in use by the licensed owners. These gaps change with time and geographic location, and can be used for communication by secondary users. Consequently, the utilization of the spectrum is improved by opportunistic frequency reuse over the spectrum holes. CR must be technically able to autonomously resolve conflicts over spectrum access by avoiding interference with incumbent signals.

2.4 Cognitive Cycles

The main functions of a CR are to acquire information about spectral opportunities by monitoring the surrounding radio environments and to exploit those opportunities in an intelligent way while guaranteeing the normal operation of the licensed PUs. In this context, a wide range of cognitive techniques available in the literature can be broadly categorized into: (i) spectrum awareness (sensing) techniques, and (ii) spectrum exploitation (adaptation) techniques [45]. The first category of techniques are used for acquiring information about the spectral opportunities while the second category deal with the exploitation of the underutilized licensed spectrum in several ways.

Depending on the employed techniques at the CR node, different levels of awareness can be achieved. The acquired information can be spectrum occupancy over the available bands, SNR of the PU signal, channel towards the PUs, modulation and coding used by the PUs, pilot/header information in the PU transmit frame, etc.

From the spectrum utilization point of view, the greater the awareness level at the CR node, the better is the spectrum utilization. For example, if the CR node has information only about the spectrum occupancy, it can transmit only in the bands which are not occupied by the PUs at that moment. However, if the CR node can acquire information about the PU SNR, it can even transmit during PU transmission with the controlled power.

The first task is done at the transmitter side, and task two is done at both transmitter and receiver. By interacting with the radio frequency environment, these tasks form a cognitive cycle as shown in Figure 2-3.

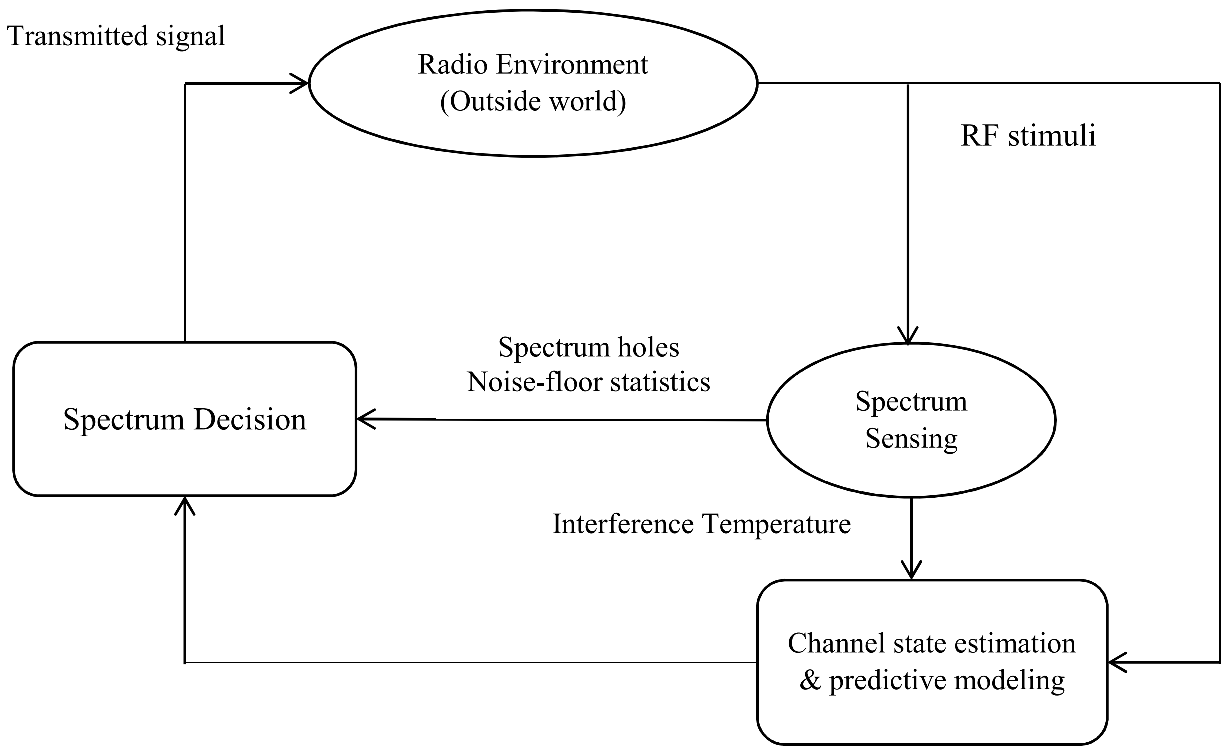

Figure 2-3 Cognitive cycle [46]

From the brief description, it is apparent that the cognitive module in both transmitter and receiver has to work in harmonious fashion. In order to maintain this condition, a feedback channel between the receiver and transmitter has to be established. Through this feedback channel, the receiver is enabled to send information on the performance of the link to the transmitter.

2.4.1 Spectrum Estimation

The first task of the CR system is to measure the wireless environment over the electromagnetic spectrum band and identifying the occupied bands, usage characteristics, and spectrum holes. As described in the previous section, this task is done so that the cognitive users can invisibly utilize the band without interfering with the licensed users. The main challenge of this task is in the identification and detection of primary user signals among the noisy radio environments. In this section we give a brief highlight on a few spectrum sensing techniques available [47-49].

2.4.1.1 Matched Filter Detection

A matched filter is a linear filter designed to provide the maximum SNR at its output for a given transmitted waveform. Figure 2.4 depicts the block diagram of matched filter. The signal received by CR is input to matched filter which is $r(t) = s(t) + n(t)$. The matched filter convolves $r(t)$ with $h(t)$ where $h(t) = s(T - t + \tau)$. Finally the output of matched filter is compared with a threshold λ to decide whether the primary user is present or not.

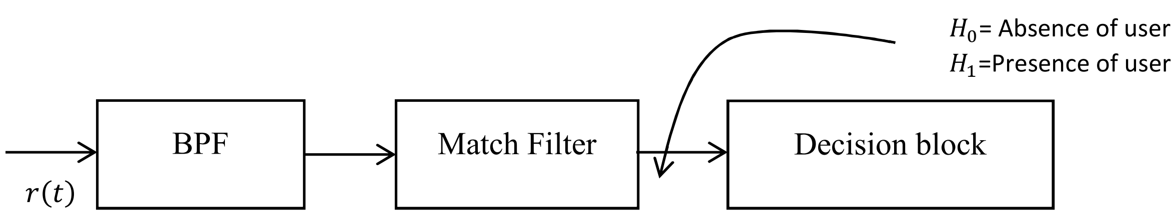

Figure 2.4 Block diagram of matched filter.

A Matched filter is an optimal detector in an AWGN channel if the waveform of primary user is previously known by CR. It means that CR should have knowledge about the waveform of primary user such as modulation type and order, the pulse shape and the packet format. So if CR doesn't have this type of prior information then it's difficult to detect the primary user. We can still use matched filter detection because in most of the communication networks we can achieve this coherency by introducing pilots, preambles, synchronization word, or spreading codes in the waveform of primary users. Still there are limitations in matched filter because each CR should have the information of all the primary users present in the radio environment. Advantage of matched filter is that it takes less time for high processing gain. However major drawback of Matched Filter is at a CR would need a dedicated receiver for every primary user class.

2.4.1.2 Energy Detection

If CR cannot have sufficient information about primary user's waveform, then the matched filter is not the optimal choice. However if it is aware of the power of the random Gaussian noise, then energy detector is optimal. In [47] the authors proposed the energy detector as shown in Figure 2.5. The input band pass filter selects the center frequency f_s and bandwidth (B) of interest. The filter is followed by a squaring device to measure the received energy then the integrator determines the observation interval *T*. Finally the output of the integrator, $y(t)$ is compared with a threshold, λ to decide whether primary user is present or not.

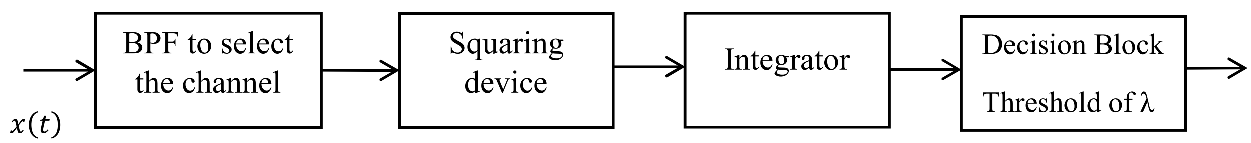

Figure 2.5 Block diagram of energy detector

One of the main problems of energy detection is that performance is susceptible to uncertainty in noise power. It cannot differentiate between signal power and noise power rather it just tells us about absence or presence of the primary user.

2.4.1.3 Cyclostationary Feature Detection

It exploits the periodicity in the received primary signal to identify the presence of primary users. The periodicity is commonly embedded in sinusoidal carriers, pulse trains, spreading code, hopping sequences or cyclic prefixes of the primary signals [49]. Due to the periodicity, these Cyclostationary signals exhibit the features of periodic statistics and spectral correlation, which is not found in stationary noise and interference.

Thus, cyclostationary feature detection is robust to noise uncertainties and performs better than energy detection in low SNR regions. Although it requires a priori knowledge of the signal characteristics, cyclostationary feature detection is capable of distinguishing the CR transmissions from various types of PU signals. This eliminates the synchronization requirement of energy detection in cooperative sensing. Moreover, CR users may not be required to keep silent during cooperative sensing and thus improving the overall CR throughput. This method has its own shortcomings owing to its high computational complexity and long sensing time. Due to these issues, this detection method is less common than energy detection in cooperative sensing.

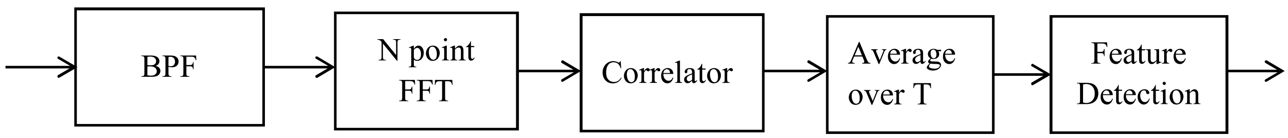

Figure 2.6 Cyclostationary feature detector block diagram

The comparison of different transmitter detection techniques for spectrum sensing and the spectrum opportunities as it is evident from the criteria, that matched filter based detection is complex to implement in CRs, but has highest accuracy. Similarly, the energy based detection is least complex to implement in CR system and least accurate compared to other approaches. The other approaches are in the middle of these two.

2.4.1.4 Polarization Based Detection

We know that conventional methods primary makes use of amplitude, frequency, and phase information of the signal for efficient detection. However the sensing performance of the conventional methods is highly degraded due to polarization mismatch between the transmitted electromagnetic wave vectors and receiving antenna polarization vector. Different from other sensing techniques polarization based detection makes use of vector nature of electromagnet signal and can further improve the sensing performance. Although it is possible to compare performance of these two different sensing techniques, but spectrum sensing is not the focus of this thesis.

2.4.2 Spectrum Adaptation

After we derived the information about the spectrum holes or usage characteristics, the next step of cognitive cycle is to adapt the system parameters based on the condition of the RF environment. This is required because the CR operates in communication environments with intensive interferences.

It can be embedded into a CR system in various aspects of its design varying from network planning, radio resource management, Medium Access Control (MAC) to physical layer signal processing schemes. The latest is commonly known as IC technique. The aim of introducing IC techniques at CR architecture is to successfully operate under high levels of interference from PUs systems and to protect PUs from secondary interference.

In the previous works several IC techniques have been developed for application at receiver and transmitter of CR architecture [14-16]. Such as, filter-based approach, transmit-and-receive beamforming, cyclostationarity-based approach, higher orders statistics-based approach, and antenna system characteristics. All these methods can be combined and implemented with each other. Some of robust spectrum adaptation techniques in the CR are listed in Figure 2.7.

The aforementioned IC techniques can all be applied for CR networks at both receiver and transmitter. Almost all IC techniques are proposed and discussed based on studies of CR transmission and reception in the signal domain, transform domain, frequency domain, waveform domain and space domain. In this thesis our work focuses on the use of combined polarization-and-spatial domain to the uplink of CR-BS system.

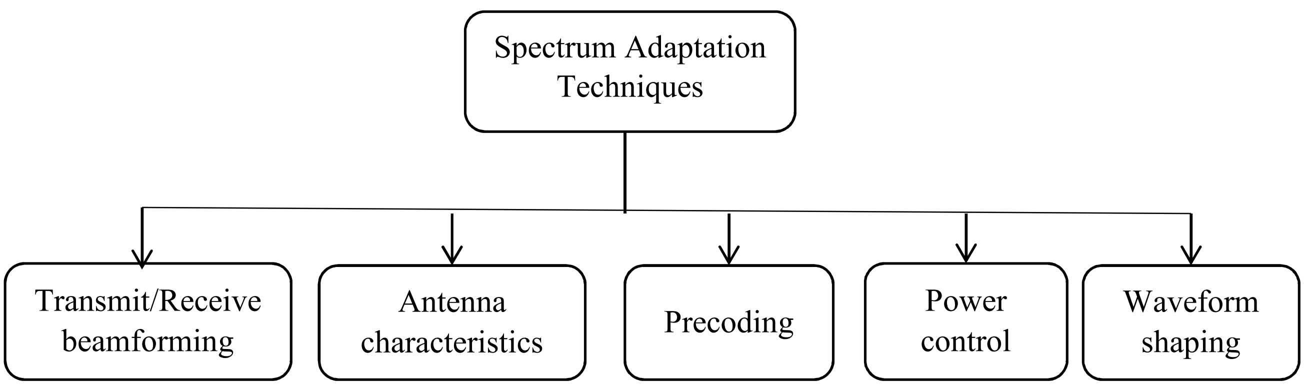

Figure 2.7 Spectrum adaptation techniques at transmitter and receiver

2.5 CR Applications

Since cognitive radios can sense, monitor and detect surrounding environment and change its operating parameters to best match the operating conditions they are used to increase the spectrum efficiency and support higher bandwidth services. Thus applications are often included in the definition of CR. Similarly due to cognitive capabilities the burden of centralized spectrum management is greatly reduces.

In today's world where there is plethora of wireless devices and technologies CR has many applications. Some of the applications are listed below:

- Improving spectrum utilization & efficiency
- Improving link reliability
- Less expensive radios
- Advanced network topologies
- Enhancing software defined radio (SDR) techniques & Automated radio resource management

CHAPTER THREE

EXISTING MODELS FOR ARRAYS AND BEAMFORMING

2.2 INTRODUCTION

Array beam forming techniques exist that can yield multiple, simultaneously available beams. The beams can be made to have high gain and low sidelobes, or controlled beamwidth. Adaptive beam forming techniques dynamically adjust the array pattern to optimize some characteristic of the received signal. In beam scanning, a single main beam of an array is steered and the direction can be varied either continuously or in small discrete steps.

Antenna arrays using adaptive beamforming techniques can reject interfering signals having a DOA different from that of a desired signal. Antenna arrays of diverse polarization using adaptive signal processing can also reject interfering signals having different polarization states from the desired signal, even if the signals have the same DOA.

An array consists of two or more antenna elements that are spatially arranged and electrically interconnected to produce a directional radiation pattern. The interconnection between elements, called the feed network, can provide fixed phase to each element or can form a phased array. In optimum and adaptive beamforming, the phases (and usually the amplitudes) of the feed network are adjusted to optimize the received signal. The geometry of an array and the patterns, orientations, and polarizations of the elements influence the performance of the array.

In section 3.2 the concepts of antenna arrays, array parameters, polarization, and signal model of Uniform Linear Array (ULA) along with its signal model are presented. The basic principles of beamforming, optimum beamforming criteria and types of beamforming are described in section 3.3. In section 3.4, review of some of well-known adaptive beamforming algorithms are presented. Finally in section 3.5 Matlab simulations and result discussions are presented.

3.2 Antenna Arrays

An antenna array is a set of antenna elements arranged in space whose outputs are combined to give an overall antenna pattern that can differ from the pattern of the individual elements [10]. An array can achieve the same directional performance of a larger antenna by trading the electrical problems of combining several antenna outputs for the mechanical problems of supporting and turning a large antenna. By varying the phase and amplitude of the individual element outputs before combining, the overall array pattern can be steered in the desired user's direction without physically moving any of the individual elements. The overall radiation pattern of an array is determined by the radiation pattern of the individual elements, their positions, orientations in space, and the relative phase and amplitudes of the feeding currents to the elements.

By the principle of pattern multiplication, the overall radiation pattern form is found as the product of the individual element's radiation patterns with the array factor. The array factor is in turn determined by the relative positions of the elements in space as well as the relative phase and amplitude levels of the feeding currents to the elements. An array of antenna performs better compared to the single antenna element. It can steer the beams and put nulls in the desire and interfere point accordingly the need of the user. Arrays of antennas can have any geometric shapes such as: linear, planar and circular as shown in figure 3.1 below.

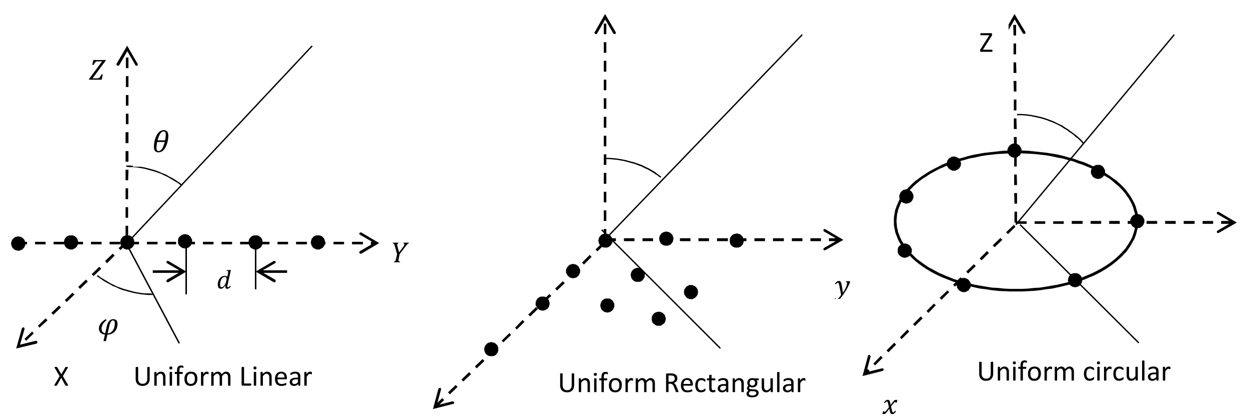

Figure 3.1Antenna array configurations.

3.2.1 Array Factor

The array factor represents the gain of the array in a particular direction. The array factor $g(\theta, \varphi)$ is a function of the azimuthal and elevation angles. The array factor of an antenna array is determined by the weighting applied to each antenna and the geometry of the array.

3.2.2 Element Numbers

The array factor of an adaptive array can be controlled with the number of elements. Generally, the more elements it has, the better the performance. By increasing the number of elements, the array factor has more sidelobes but their levels are lower. This improves directionality and interference is cancelled more effectively. The number of nulls is increased and they are deeper. The beams are narrower and the gain of the array is higher because of spatial diversity. The number of elements possible is constrained by a cost and physical limitations.

3.2.3 Element Polarization

An important antenna parameter for efficient communication from antennas to antenna is polarization. The polarization of the EM field describes the orientation of its vectors at a given point and how it varies with time. In other words, it describes the way the direction and magnitude of the field vectors (usually E) change in time. Transverse Electromagnetic (TEM) wave propagation consists of two parts, the electric and magnetic field components, which oscillate in phase perpendicular to each other and perpendicular to the direction of propagation. Behaving in accordance with the Maxwell's equations, the oscillation of the electric field induces a magnetic field, which the magnetic field itself oscillates to regenerate the electric field and so on. These oscillations between the two fields then store energy which is carried along the direction of propagation [45]. Figure 3.2 illustrates the propagation of electromagnetic wave with respect to a single polarization antenna located at a reference point. The electric and magnetic field components are oscillating on the plane described by the unit vectors u_θ and u_ϕ; where the plane is perpendicular to the direction of propagation along the direction u_r. In this spherical coordinate system, the parameter θ denotes an azimuth angle, measured anticlockwise from the positive x-axis, while ϕ represents an elevation angle, measured anticlockwise from the x-y plane, as shown in the figure.

Using a spherical coordinate system formed by the directional unit vectors u_r, u_θ and u_ϕ; the electric field component vector E can be written as

$$E = E_\theta u_\theta + E_\phi u_\phi, \tag{3.1}$$

where E_θ and E_ϕ denote the field strengths along the vectors u_θ and u_ϕ respectively. The amplitude of the field is given by

$$\|E\| = \sqrt{E_\theta^2 + E_\phi^2} \tag{3.2}$$

It should be noted that the magnetic field component can be expressed in the same fashion, but 90^0 out of phase. For the sake of simplicity, only electric field is considered here.

To characterize the field oscillation, the polarization ratio is defined as the ratio between E_{ϕ} and E_{θ}; given as [51]

$$Polarization\,ratio \triangleq \frac{E_{\phi}}{E_{\theta}} = \tan\gamma\exp(j\eta), \tag{3.3}$$

where the parameters $0 \leq \gamma \leq \frac{\pi}{2}$ and $-\pi \leq \eta \leq \pi$ denote the auxiliary polarization angle and the polarization phase difference respectively. Through observing the polarization ratio, different states of polarization can be defined, as shown in Figure 3.3.

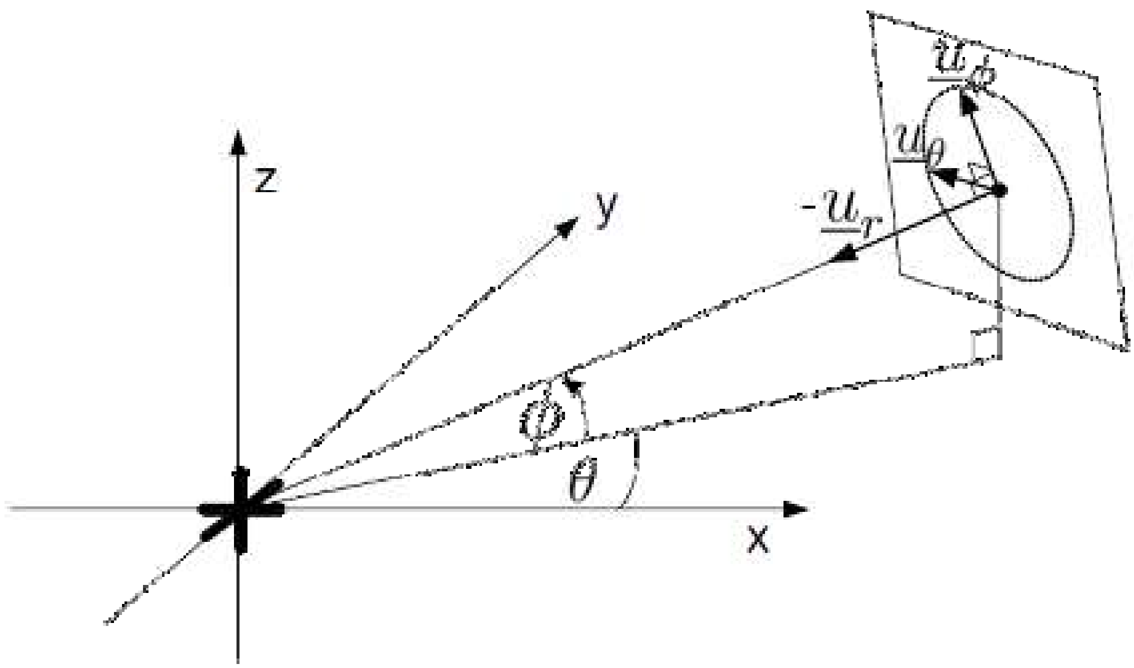

Figure 3.2: Geometry of the TEM wave propagating to a single antenna located at the reference point [50].

The signal is said to be in a linear polarization state if the polarization ratio is constant at any time (i.e. the field vector moves back and forth along a line). This includes vertical ($E_{\theta} = 0$); and horizontal $\left(E_{\phi} = 0\right)$ polarizations. Meanwhile, the signal is in circular polarization state if the components E_{θ} and E_{ϕ} share the same magnitude but 90^{0} out of phase. The field vector remains constant in length, but circularly rotates around the polarization plane. In the most general cases, the signal is in elliptical polarization state, where the components E_{θ} and E_{ϕ} do not have the same magnitude. A signal can be either left-hand or right-hand polarized depending on the rotation direction of the field [50].

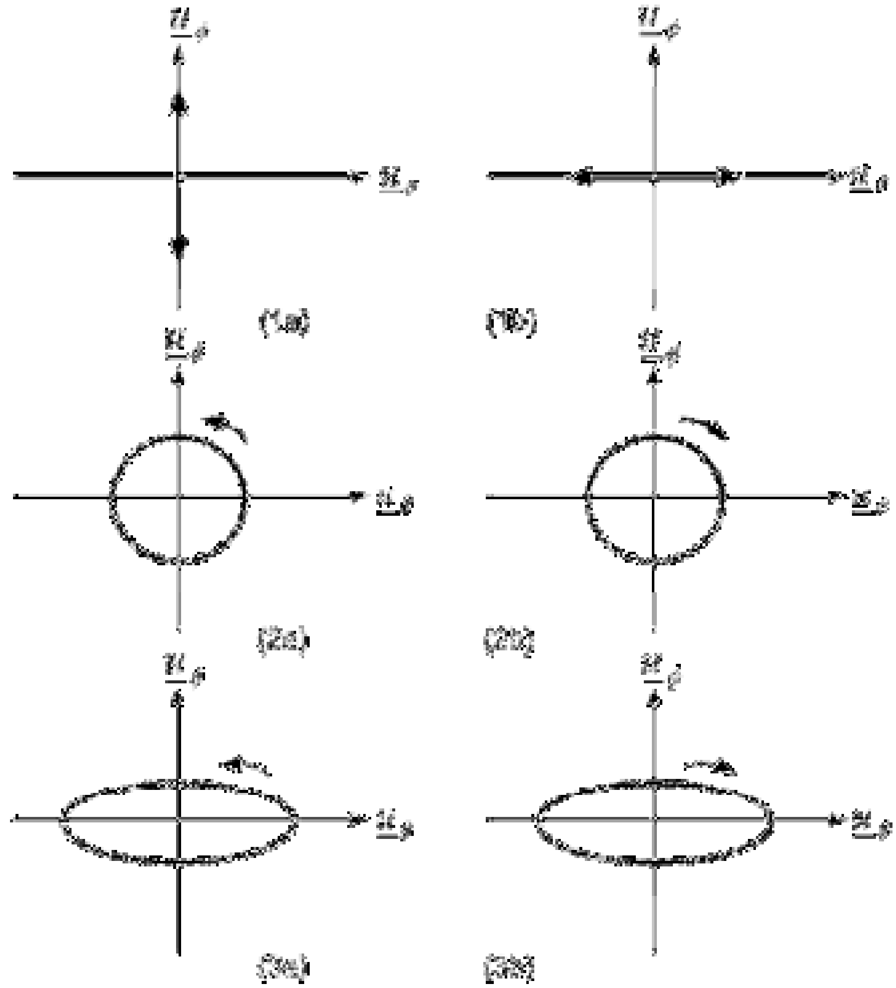

Figure 3.3 Different states of polarization (1a) vertical (1b) horizontal (2a) right-hand circular (2b) left-hand circular (3a) right-hand elliptical (3b) left-hand elliptical. [51]

It should be noted that only a completely polarized wave, where the polarization state is fixed at all time, is considered in this thesis. The modulation of random noise onto a carrier wave can fluctuate, the components E_θ and E_ϕ. If the resultant field is completely uncorrelated, the wave is said to be completely unpolarized. Meanwhile, the wave is partially polarized, where the field is expressed as the sum of the completely polarized and completely unpolarized.

3.2.4 Signal Model of ULA Array

One of the simplest geometries for an array is a linear array in which the centers of the antenna elements are aligned along a straight line are used here. Consider an N-element uniformly spaced linear array with element spacing d which is illustrated in Figure 3.4. Suppose that there are M

narrowband far field plane wave signals $s_1(t), s_2(t), \ . \ . \ ., s_M(t)$ impinging up on the array with a DOA θ_i, for $i = 1,2, . \ . \ ., M$. Also assume that the signals propagates in a homogeneous media and that the array consists of identical distortion-free Omni-directional elements. The time-delay τ between two adjacent sensors for the input signal with known DOA angle θ is expressed as

$$\tau(\theta_i) = \frac{(i-1)d\sin\theta}{c} \tag{3.4}$$

where c is the propagation speed of the wavefront. In general, the incident signal $s(t)$ with time delay τ between receiving elements can be written as $s(t-\tau)$. If $s(t)$ is a narrowband signal, $s(t-\tau)$ can be simply approximated by a phase shift of $s(t)$, that is, $s(t-\tau) = s(t)e^{j2\pi f_0\tau}$, where f_0 is the central frequency of $s(t)$. Since we adopt the narrow band assumption, it is needed that over the relative bandwidth B and for limited sizes of the array aperture (i.e., the physical size of the antenna array measured in wavelengths) the condition should be satisfied that $B\tau \ll 1$, meaning that τ is much less than the inverse of the relative bandwidth.

The signal induced on the k^{th} element due to the i^{th} source can be expressed as

$$x_k(t) = s_i(t)e^{j2\pi f_o(t-\tau(\theta_i))} \tag{3.5}$$

Then, the received signal at the array is a superposition of all the impinging signals and noise. Therefore, the overall input data vector may be expressed as

$$\mathrm{x}(t) = \sum_{i=1}^{M} \mathrm{a}(\theta_i)s_i(t) + n(t) \tag{3.6}$$

where $\mathrm{a}(\theta_i)$ is the array steering vector and given by,

$$\mathrm{a}(\theta_i) = \begin{bmatrix} 1 \\ e^{-jkd\sin\theta_i} \\ \vdots \\ e^{-j(N-1)kd\sin\theta_i} \end{bmatrix} \tag{3.7}$$

and $\mathrm{n}(t)$ denotes the $N \times 1$ vector of the noise at the array elements, and $k = 2\pi/\lambda$ is the wave number.

In matrix notation, equation (3.6) becomes

$$\mathrm{x}(t) = \boldsymbol{A}(\boldsymbol{\Theta})\mathrm{s}(t) + \mathrm{n}(t) \tag{3.8}$$

where, $\boldsymbol{A}(\boldsymbol{\Theta})$ is the $N \times M$ matrix of the steering vectors, and written as

$$\boldsymbol{A}(\boldsymbol{\Theta}) = [\mathrm{a}(\theta_1), \mathrm{a}(\theta_2), \ldots, \mathrm{a}(\theta_M)] \tag{3.9}$$

and

$$s(t) = [s_1(t), s_2(t), \cdots, s_M(t)]^T \tag{3.10}$$

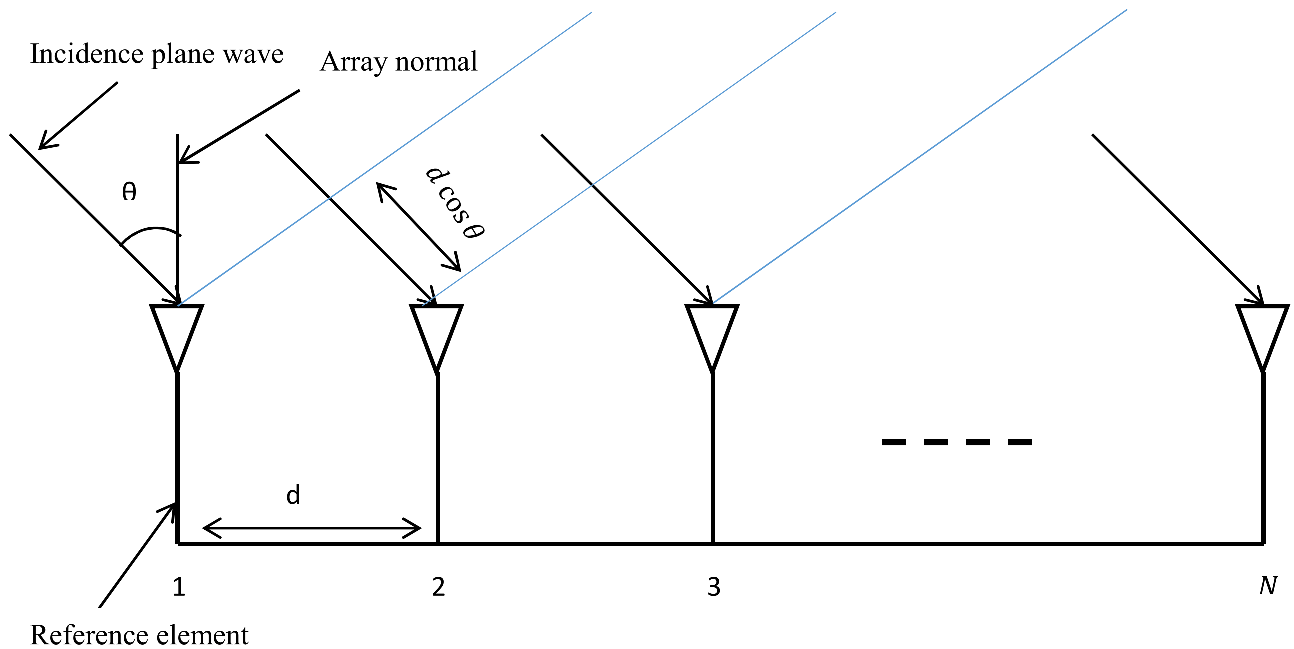

Figure 3.4 ULA array model.

3.3 Beamforming

In the 1960s, beamforming was introduced in order to remove unwanted noise from military Sonar and Radar systems. Since then it has been studied in many areas such as seismology, communications, imaging, geophysical exploration, and acoustic source localization etc. Signals propagating in space or three dimensions by nature encounter the presence of noise and interference. In many applications, there is a need to separate the multiple sources or extract a source of interest while minimizing undesired interfering signals and noise [9]. If the signals are separated in frequency band temporally they can be separated from harmful effects of noise and interference. But if they occupy the same temporal frequency band then we have to use some kind of separating mechanism to avoid the effect of noise and interference. Since in many situations the desired signal and the interferences originate from different locations in space or three dimensions, the signals can be separated by exploiting the spatial separation.

A Beamformer is a processor used in conjunction with an array of sensors (i.e., antenna elements in an adaptive array) to provide a versatile form of spatial filtering. The sensor array collects spatial samples of propagating wave fields, which are processed by the beamformer. Typically a beamformer linearly combines the spatially sampled time series from each sensor to obtain a scalar output time series in the same manner that an FIR filter linearly combines temporally sampled data. Some of the uses of beamforming are signal detection, controlling direction of arrival (DOA) of signal, and maximizing signal which is corrupted by noise, competing sources, and reverberation in the intended direction. A Beamformer consists of an array of sensors and adaptive algorithm as shown in figure 3.5.

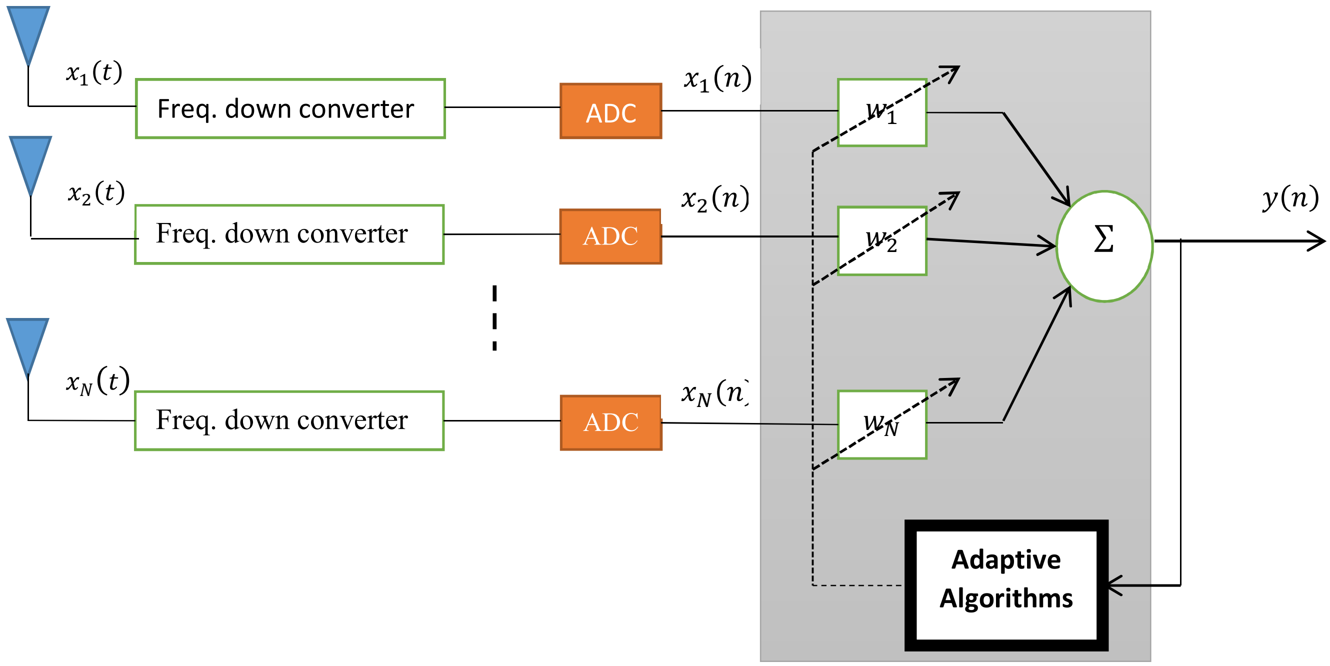

Figure 3.5 Adaptive antenna array models

The output of the adaptive antenna array $y(n)$ can be given by:

$$y(n) = \sum_{n=1}^{N} w_n \, x_n(n) \tag{3.11}$$

where, w_n is the complex weight of the antenna element n, for $n = 1, 2, 3, \ldots, N$. The above equation may also be written in vector form as

$$y(n) = w^H \mathrm{x}(n) \tag{3.12}$$

where

$$w = [w_1 \; w_2 \; \ldots \; w_N]^T \tag{3.13}$$

and $(.)^H$ denotes the Hermitian (complex-conjugate) transpose. The vector w is $N \times 1$ complex weight vector. In general, to apply beamforming algorithms, the numerical dimension of the space spanned by $\mathrm{a}(\theta_i)$ should be less than N to be able to solve the matrix equations. In other words, the number of signals impinging on the array antenna is required to be less than the number of array elements, i.e. $M < N$.

The important performance parameter of antenna array is array factor and given by;

$$g(\theta) = w^H \mathrm{a}(\theta) \tag{3.14}$$

where, $g(\theta)$ represents the response of the array to a signal with DOA equal to θ. So if there are several signals coming from different directions, and we want to extract the signal with direction θ_i, we need to find a set of weights such that the array response has a higher gain at direction θ_i, and lower gains (or ideally nulls) at other directions. Where w and $\mathrm{a}(\theta_i)$ are defined in equation (3.13) and (3.7), respectively. In the equations above the weight vector w is a function of the steering vector(s); the steering vector depends on the incident angle θ.

The beampattern is defined as the magnitude of $g(\theta)$ [15] and is given by

$$G(\theta) = |g(\theta)| \tag{3.15}$$

Using $G(\theta)$, we may define the normalized beamformer response,

$$g_n(\theta) = \frac{g(\theta)}{\max\{G(\theta)\}} \tag{3.16}$$

where $g_n(\theta)$ is also known as the normalized radiation pattern or array factor of the array.

The signal to interference plus noise ratio (SINR) has the following form

$$SINR = \frac{w^H R_{xx} w}{w^H R_{i+n} w} \tag{3.17}$$

where R_{xx}, represents the data spatial covariance matrix of the received data samples given by

$$R_{xx} = E[\mathrm{x}(n)\mathrm{x}^H(n)] \tag{3.18}$$

and R_{i+n} is signal plus noise covariance matrix.

3.3.1 Optimal Beamforming Criteria

The weight coefficient w**,** may be pre-assigned or assigned based on the statistics of data and leads to either fixed or adaptive beamforming methods. In the fixed beamforming techniques the weight coefficients are pre-assigned and do not updated during operation. On the other hand, the values of weight coefficients in adaptive algorithms are assigned based on statistics of the received data and thus preferable for CR technology.

Complex weights for each element of the array can be calculated to optimize some criteria of the received signal. The most common performance criteria are: Mean Square Error (MSE), Maximum likelihood (ML), Maximum Signal to Noise Ratio (MSNR), and Maximum Signal-to-

Interference Noise Ratio (MSINR). This does not always result in an array pattern having a beam maximum in the direction of the desired signal but does yield the optimal array output signal. Most often this is accomplished by forming nulls in the directions of interfering signals.

3.4 Adaptive Algorithms

Adaptive beamforming is an iterative approximation of optimum beamforming. In general, it adjusts the weight vector such that it places deep nulls in the direction of interfering signals in an attempt to maximize the SINR at the Beamformer output. There are two major classes of adaptive beamforming algorithms based on their requirements for training signal sequence: non-blind and blind adaptive algorithms [10, 19, and 20].

Non-blind adaptive algorithms require statistical knowledge of the transmitted signal in order to optimize the array weights. In other words, to extract the desired user(s) from the surrounding environment (or received signals) a training signal sequences which are known both at the receiver and transmitter are transmitted. Then based on the information obtained from the received signal the array weights are optimized (adjusted) to reduce the error between the received signal sequences and the known transmitted signal sequences at the receiver. The Least Mean Square (LMS), Sample Matrix Inversion (SMI) and Recursive Least Square (RLS) are some of the non-blind adaptive algorithms.

Unlike non-blind algorithms, blind algorithms do not require training signal sequences rather they try to estimate information from the received signal. CMA and LSCM are some examples of blind adaptive beamforming algorithms. To exploit the advantages of adaptive antenna array fully for time-varying environment and extend its use to the new emerging CR technology, we have to examine some of robust adaptive beamforming techniques used by the existing wireless communication.

3.4.1 Least Mean Square (LMS) Algorithm

Least Mean Square (LMS) algorithm is a non-blind adaptive beamforming algorithm which searches for optimal weights that would minimize the Mean Square Error (MSE). Through a feedback loop, the weights $w_1, w_2, \ldots, w_N$ are updated by the adaptive processor that has the time sampled error signal, $e(n)$ as input, given by:

$$e(n) = d(n) - y(n) \tag{3.19}$$

Substituting for $y(n)$ from equation (3.12) the error data is equivalently written as

$$e(n) = d(n) - w^H x(n) \tag{3.20}$$

where, $d(n)$ is the training sequence, $y(n)$ is the output of the adaptive beamformer and $x(n)$ is the input signal vector to the array as defined in previous section. Then, the mean squared error (MSE) is given by:

$$MSE = E\{|e(n)|^2\} \tag{3.21}$$

where $E\{.\}$ is the expectation operator.

Substituting equation (3.20) in to equation (3.21) and expanding the augment of the MSE term;

$$E[|e(n)|^2] = E[\{d(n) - w^H(n)x(n)\}\{d[n] - w^H(n)x(n)\}^*] \tag{3.22}$$

The above equation of MSE is called the performance surface or cost function, which forms a quadratic surface in the M dimensional space [29]. Since the optimum weights must provide the minimum MSE, the extremum is the minimum of the cost function [28]. The minimum value is obtained by taking the gradient of cost function with respect to the weight vectors and equating it to zero

$$\nabla_{\mathbf{w}}(MSE) = 2R_{xx}(n)w(n) - 2r_{xd}(n) = 0 \tag{3.23}$$

where,

$$R_{xx} = E[x(n)x^H(n)] \tag{3.24}$$

$$r_{xd} = E[x(n)d^*(n)] \tag{3.25}$$

are the instantaneous estimate of the self-correlation between the signal induced in each array element and the cross correlation between the reference signal and the induced signal respectively. Solution for the weights is called optimum Weiner solution and is given by:

$$w_{opt} = R_{xx}{}^{-1} r_{xd} \tag{3.26}$$

The LMS algorithm avoids matrix inverse operation by using the instantaneous performance gradient vector to update the weight vector.

The steepest descent iterative approximation is given as

$$w(n+1) = w(n) - \frac{1}{2}\mu\nabla_{\mathbf{w}}(MSE) \tag{3.27}$$

where μ is the convergence factor which controls the speed of convergence and its value is usually between 0 and 1. If these values are substituted in the gradient of performance surface we can get the LMS solution.

$$w(n+1) = w(n) - \mu(R_{xx}w - r_{xd}) \quad (3.28)$$

The computation of matrix associated with the Steepest Descent Method is another problem of this method. To overcome this difficulty, the LMS algorithm replaces the auto-correlation and cross-correlation by their instantaneous values instead of their actual values. Therefore, Eq.3.28 can be rewritten as [30]:

$$w(n+1) = w(n) + \mu\, x(n)e^*(n) \quad (3.29)$$

Much iteration is required for the LMS algorithm for convergence of the weight vector. Hence, LMS algorithm converges slowly [20].

3.4.2 Sample Matrix Inversion (SMI) Algorithm

One of the drawbacks of the LMS algorithm is the rate of convergence of weights is slow since it must go through many iterations before satisfactory convergence is achieved. So we have another algorithm called Sample Matrix Inversion (SMI) algorithm. The idea of SMI algorithm is to estimate the correlation matrix R_{xx} and the cross-correlation vector r_{xd} based on the samples of the array sensor input in an observation interval so that the speed of convergence is improved. Since we do not have the true auto-correlation matrix and cross-correlation vector, this algorithm replaces both of them by their corresponding estimations (time averaging) to obtain the Wiener-Hopf solution. The sample estimations are given by [20]:

$$\hat{R}_{xx} = \frac{1}{K}\sum_{n=1}^{K} x(n)x^H(n) \quad (3.30)$$

$$\hat{r}_{xd} = \frac{1}{K}\sum_{n=1}^{K} x(n)d^*(n) \quad (3.31)$$

In this algorithm, the input samples are divided into "k" number of blocks and each number of blocks is of length K. Since we use a K-length block of data, this method is called a block-adaptive approach.

In terms of the above estimations the Wiener-Hopf solution becomes [20]

$$\bar{w}_{opt} = \hat{R}_{xx}^{-1}\hat{r}_{xd} \quad (3.32)$$

As the block size increases the time average values better approximate the ensemble, resulting in a minimized estimation error in such a way that a much more closer solution to the Wiener-Hopf is obtained.

3.4.3 Recursive Least Square (RLS) Algorithm

Recursive Least Square (RLS) Algorithm is a non-blind adaptive beamforming algorithm that uses the Least Square criterion for optimization. This algorithm tries to achieve the faster convergence of SMI while overcoming its computational complexity and potential singularities by computing the array correlation matrix and correlation vector recursively [21]. The correlation matrix and the correlation vector used in SMI algorithm uses rectangular windows of equal width, which considers all previous time samples equally. Since the signal sources can change or slowly move with time, RLS deemphasizes the earlier data samples and emphasize the most recent ones to compute the weighed estimate of $\hat{R}_{xx}(n)$ and $\hat{r}(n)$ [20]. This reduces the computational complexity. The weighted estimates are calculated by the iterative expressions given by:

$$\hat{R}_{xx}(n) = \alpha\hat{R}_{xx}(n-1) + x(n)x^H(n) \tag{3.33}$$

$$\hat{r}(n) = \alpha\,\hat{r}(n-1) + d^*(k)x(n) \tag{3.34}$$

where, α is a forgetting factor such that $0 \leq \alpha \leq 1$.

Sherman-Morrison-Woodbury (SMW) equation is used to compute the inverse of $\hat{R}_{xx}(k)$, i.e.

$$\hat{R}_{xx}^{-1}(n) = \alpha^{-1}\hat{R}_{xx}^{-1}(n-1) - \frac{\alpha^{-2}\hat{R}_{xx}^{-1}(n-1)\bar{x}(n)\bar{x}^H(n)\hat{R}_{xx}^{-1}(n-1)}{1+\alpha^{-1}x^H(n)\hat{R}_{xx}^{-1}(n-1)x(n)} \tag{3.35}$$

The optimum weights are given by the iterative equation:

$$w(n) = w(n-1) + \bar{g}(n)[d^*(n) - x^H(n)w(n-1)] \tag{3.36}$$

where, the gain vector $\bar{g}(k)$ is defined as:

$$\bar{g}(n) = \frac{\alpha^{-1}\hat{R}_{xx}^{-1}(n-1)x(n)}{1+\alpha^{-1}x^H(n)\hat{R}_{xx}^{-1}(n-1)x(n)} \tag{3.37}$$

3.4.4 Constant Modulus Algorithm (CMA)

Constant Modulus Algorithm (CMA) is a blind adaptive beamforming algorithm, which uses the constant modulus property of the transmitted signal to make an optimum beam to the intended direction instead of using a training signal sequence. The receiver restores the envelope of the transmitted signal by equating the received signal to some constant value that corresponds to the envelope of the transmitted signal. This is made possible by continuously updating the weight of the beamformer until the output of the array has the same modulus as that of the original transmitted signal [19, 21]. The cost function $J(k)$ used for CMA is given by:

$$J(n) = E[|y(n)|^p - |\alpha|^q] \tag{3.38}$$

where p = 1, 2 or q = 1, 2 and α is the desired signal amplitude at the output of the array. Assuming that $|\alpha| = 1$, the above equation becomes:

$$J(n) = E[|y(n)|^p - 1] \tag{3.39}$$

The cost function is a positive measure of the average amount of deviation of the output of beamformer, $y(n)$, from the unit modulus condition [11]. To choose the weight vector recursively that minimizes J and consequently makes $y(n)$ as close to a constant modulus signal as possible, an iterative method is used, which is based on the steepest descent method applied in LMS Algorithm [20]. The CMA equation thus becomes:

$$w(n+1) = w(n) - \frac{1}{2}\mu\nabla(J(n)) \tag{3.40}$$

Where: $\nabla(J)$ is the gradient of cost function of the CMA

The $\nabla(J)$ for $p = 1, q = 2$ becomes

$$\nabla\big(J(n)\big) = 2\frac{\partial J(n)}{\partial w^*(n)} = 2E\left[(|y(n)| - 1)\frac{\partial y(n)}{\partial w^*(n)}\right] \tag{3.41}$$

Further simplification of the above equation results:

$$\nabla\big(J(n)\big) = 2E\left[x(n)\left(y(n) - \frac{y(n)}{|y(n)|}\right)^*\right] \tag{3.42}$$

As done for the LMS, we replace the statistical expectation with the instantaneous value so that equation 3.42 becomes:

$$\nabla J(n) = 2\left(x(n)(y(n) - \frac{y(n)}{|y(n)|})^*\right) \tag{3.43}$$

Substituting Eq. 3.43 into Eq. 3.41 results in the following weight updating equation

$$w(n+1) = w(n) - \mu x(n)(y(n) - \frac{y(n)}{|y(n)|})^* \tag{3.44}$$

$$w(n+1) = w(n) - \mu\, x(n)e^*(n) \tag{3.45}$$

where μ has similar function as to LMS but we choose $\mu \ll 1$ to get better stability.

Like in the LMS algorithm, the convergence rate can be controlled by varying μ . However, to get much better convergence behavior, non-linear least square method need to be used.

3.5 Simulations and Discussion

In order to compare the performance of each of the conventional adaptive beamformers with optimum solution, a simulation using MATLAB software is carried out. In this part of simulation, the purpose is to demonstrate the performance degradation on conventional adaptive beamformers in the case of low input SNR and small angle separation between CR user and interferences. To validate the study, two different scenarios are compared with different position of interferer. The performance surfaces simulated to evaluate adaptive beamformers are the resultant beampattern and output-SINR. From the radiation pattern plot, strength of the main beampattern along the direction of the intended user, side lobe levels, and the ability of algorithms to produce a null along the direction of the interferers are studied.

A 10 element uniform linear array (ULA) with half wave-length spacing ($d = \lambda/2$) between the elements is considered. There are three users, one desired and two interferers which are assumed to impinge upon the array. All users' signals are assumed as narrowband signals in the time domain. The modulation scheme used in the system is the binary phase-shift keying (BPSK), the carrier frequency f_c is equal to 2 GHz. The AWGN model is also assumed. We have taken 1000 snapshots of data by antenna elements. Next, the details of the simulation parameters for LMS, SMI, and CMA are specified in table 3.1 below:

Table 3.1 Simulation parameters and assumptions taken

Number of antenna elements	8 or 10 (ULA)
Carrier frequency	2 GHz
Channel type	AWGN
K (number of iterations)	200
μ(convergence factor)	0.005
α(forgotten factor)	0.01
Signal to Noise Ratio (SNR)	$10\ dB\ upto\ 30\ dB$
Interference to noise ratio (SIR)	$20\ dB$
✓ Coupling is neglected ✓ Signals are far field with BPSK modulated ✓ The signals are uncorrelated	

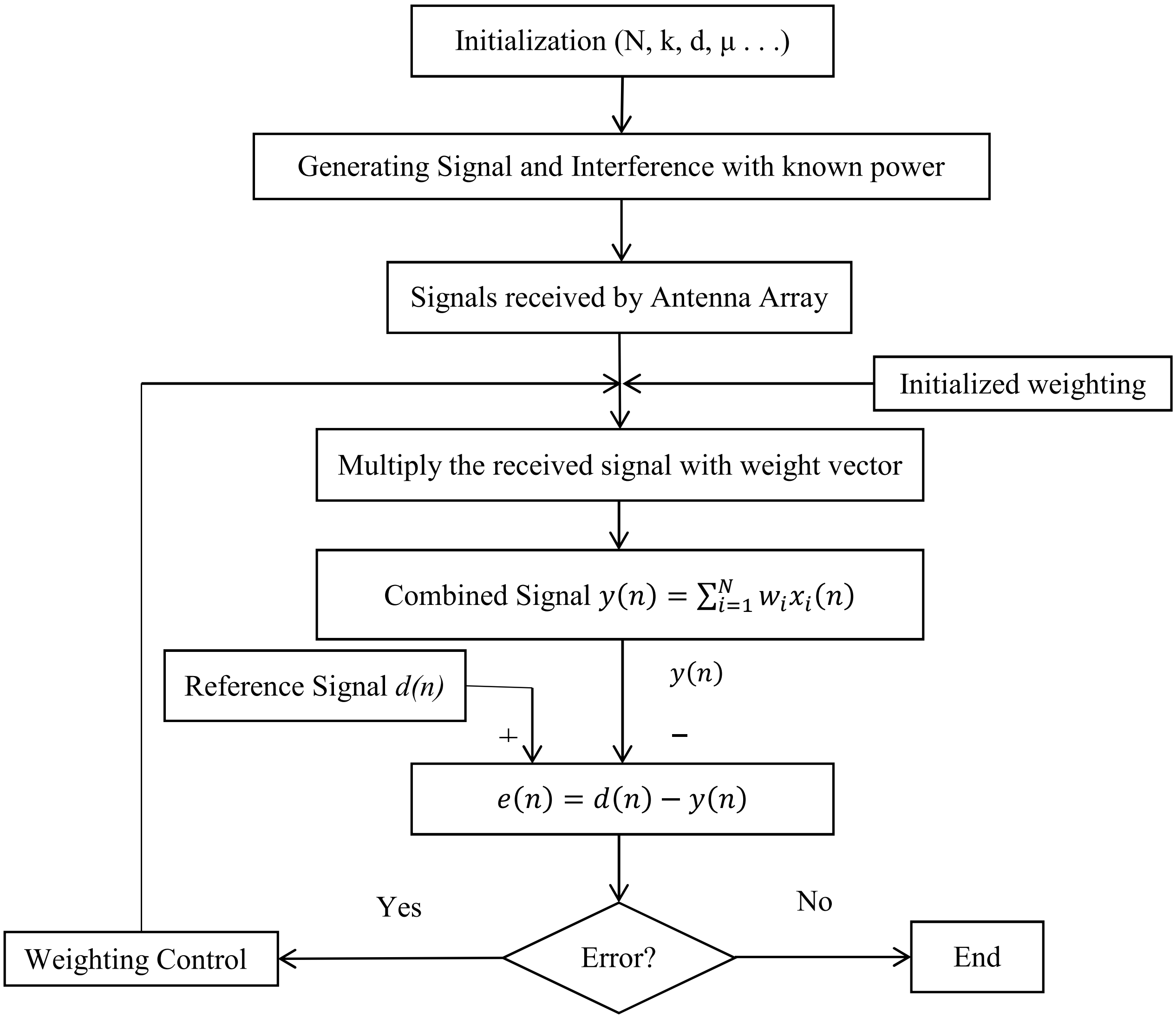

Figure 3.6 Adaptive Beamforming Flow chart.

3.5.1 Simulation Results with Large DOA Differences

In this scenario we study the resultant beam pattern and output-SINR performance of LMS, SMI, and CMA beamformers with large angle separation between desired signal and interferences. The ULA receives a desired signal arriving from angle $\theta_d = 0^0$ and two interference signals arriving from angles $\theta_{i1} = -30^0$ and $\theta_{i2} = 30^0$, with the interference-to-noise (INR) of both of them are 20 dB.

Figure 3.7 shows the plot of resultant beampatterns of SMI, LMS, and CMA algorithms with fixed CR user SNR of 10 dB. The simulation results shows that the desired user is provided with main beam at the desired 0^0 angle and nulls are given to the interferers at -30^0 and 30^0. One can observe from this result that for large angle of separation or when the separation is larger than half of the first null beam width, the side lobe level, the beam steering ability and nullifying capability of all algorithms are satisfactory. LMS produces a sharp main-beam at the desired angle and minimizes interference to a great extent compared to SMI and CMA. Convergence rate of LMS algorithm is slow compared to other algorithms. SMI algorithm also produces satisfactory main beam level and its convergence rate is fast compared to other algorithms. Also we can see that the CMA has similar behavior to that of LMS and SMI but with slow convergence rate. The convergence rate can be improved by increasing μ. However; care must be taken not to use large value of μ that renders the algorithm unstable.

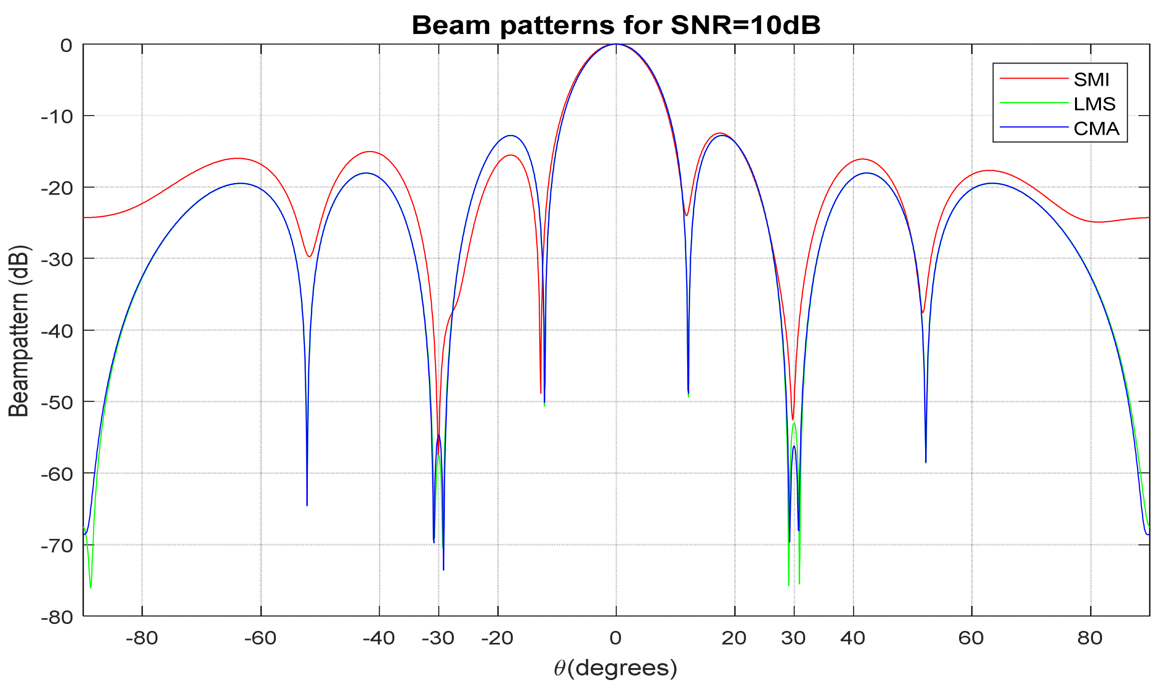

Figure 3.7 Beam patterns of LMS, SMI, and CMA algorithms for; $N = 10$, $SNR = 10\ dB$, $INR = 20\ dB$, $\theta_d = 0^0$, $\theta_{i1} = -30^0$, and $\theta_{i2} = 30^0$.

Figure 3.8 illustrate performance comparison of output-SINR versus input SNR for all mentioned conventional adaptive algorithms with similar parameters considered. For lower input SNR values the output SINR of CMA is not satisfactory. For upper values all algorithms perform well. The performance of SMI is better as compared to LMS and CMA for every values of input SNR.

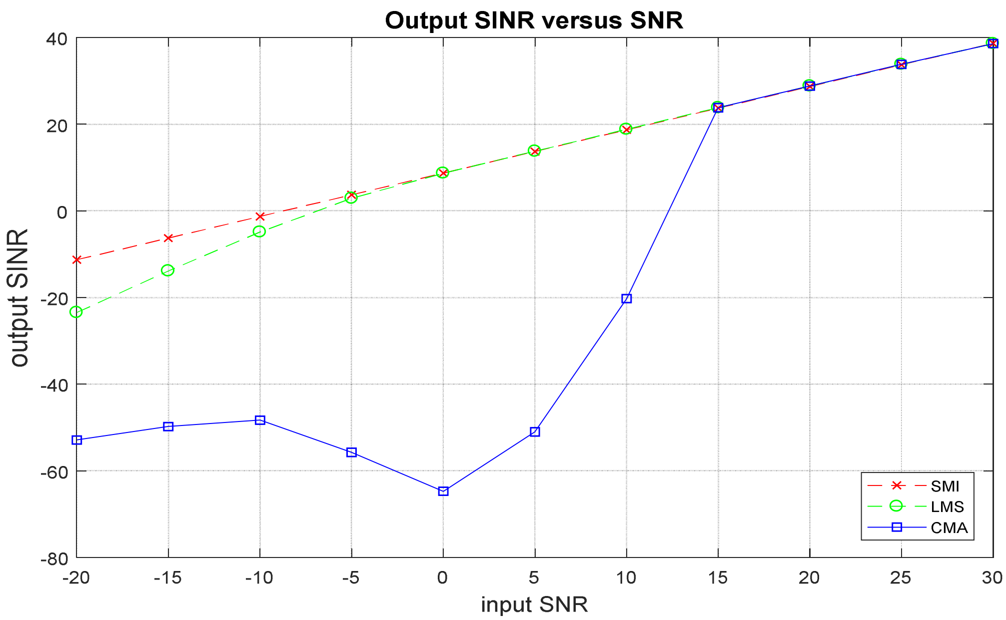

Figure 3.8 Output-SINR for SMI, LMS, and CMA algorithms.

3.5.2 Simulation Results with Small DOA Difference

In this second scenario, we again study similar performances surface of beam pattern and output-SINR for LMS, SMI, and CMA beamformers for small angle separation between desired signal and interferences. The ULA receives a desired signal in the same direction as in case one with two interference signals arriving from angles $\theta_{i1} = -30^0$ and $\theta_{i2} = 10^0$. Other simulation assumptions remain the same with those in scenario one.

Figure 3.9 shows the beampattern plot of LMS, SMI, and CMA algorithms with fixed desired user SNR of $10\ dB$. It is seen from these beampattern plot, all adaptive beamformers fails to point the main beam to desired direction at 0^0. The beamformers tried to place null toward the first interferer direction at -30^0, but they fails to place second interferer direction at 10^0. The side lobe levels are also comparable to the main lobe. These results are unaccepted in the system and should be minimized as much as possible for reliable communication. The other point which can be observed from both cases is that the speed of convergence is not affected by angle of separation but the error becomes very large until the weight converges to the optimal value.

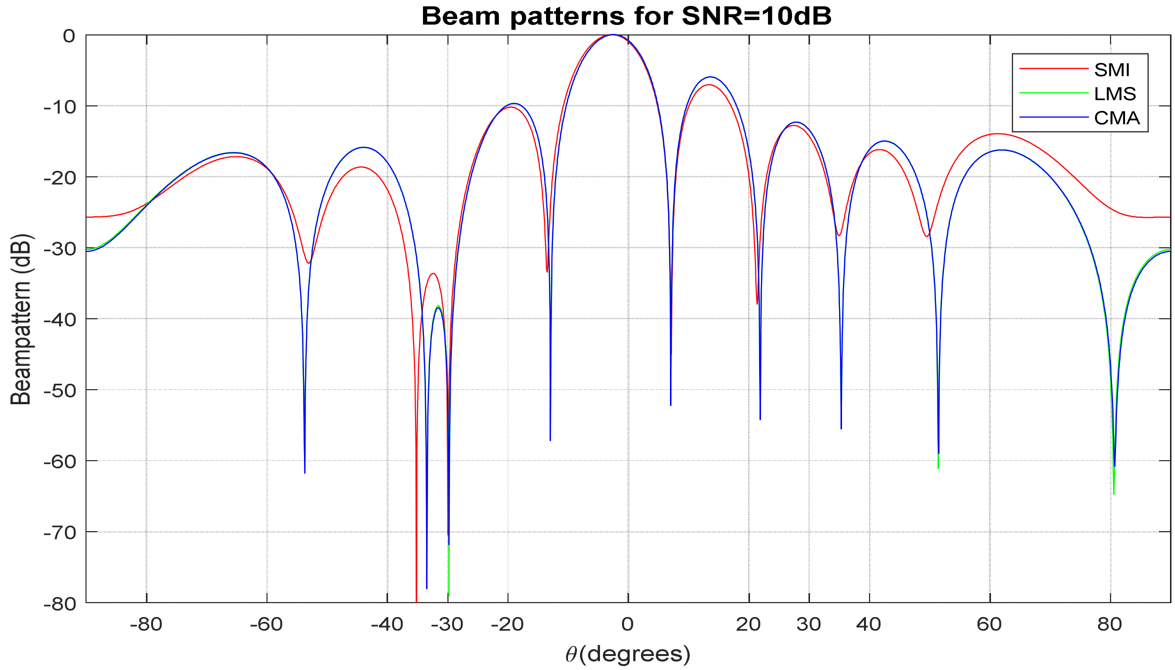

Figure 3.9 Beam patterns plots of SMI, LMS, and CMA for; $N = 10$, $SNR = 10\ dB$, $INR = 20\ dB$, $\theta_d = 0^0$, $\theta_{i1} = -30^0$, and $\theta_{i2} = 30^0$.

From the output-SINR versus input SNR plot of figure 3.10, we can see that its performance degrades as DOA separation between desired user signal and interference is small.

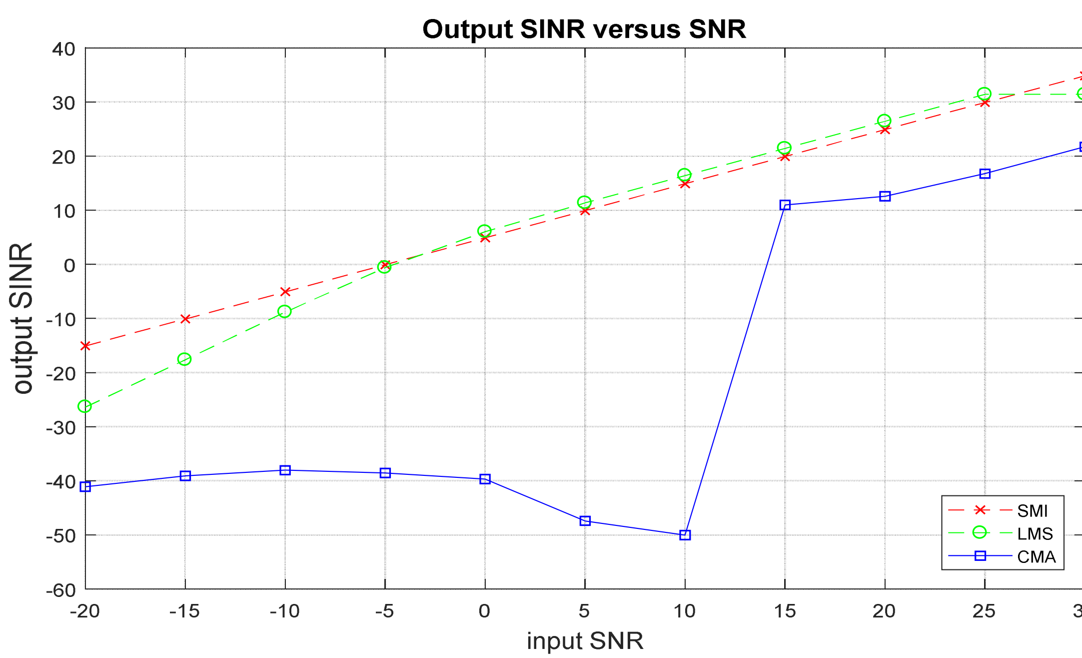

Figure 3.10 Output-SINR vs input SNR of SMI, LMS, and CMA beamformers.

3.6 Summary

We can conclude from simulation results of Figure 3.7 when the DOA separation between desired user signal and interferers is large enough, the strength of the main beampattern, side lobe levels, and nullifying capabilities of all conventional adaptive algorithms is satisfactory. The output SINR in Figure 3.8 is also acceptable. In general for large angle separations, these algorithms have satisfactory performance and can be deployed for the CR-BS system application. However from simulation results of Figure 3.9 conventional adaptive beamformers confused to direct the main beam towards the desired direction, and side lobe levels are also increased. So in wireless communication system sidelobe levels will contribute the level of interference seen by receiver when antenna arrays are used.

It is also shown from output-SINR plots of Figures 3.8 and 3.10 for a low input SNR values the performance of conventional beamformers are not satisfactory. The other important point which must be noticed is that all above simulations are performed by assuming perfectly matched polarization between receiving antenna array and imping signal. In practical sense this assumption may not work and the performance of conventional adaptive beamformers even becomes worse when polarization mismatch exists.

CHAPTER FOUR

THE PROPOSED ARRAY AND ADAPTIVE ALGORITHMS FOR UPLINK OF CR-BS

4.1 INTRODUCTION

As we have seen in chapter 3, conventional scalar array based adaptive beamformers like; LMS, SMI, RLS, CMA, and the likes can be employed by a CR-BS system as an efficient interference mitigation technique due to its spatial filtering functionality. At uplink an adaptive beamformer at the CR BS can direct main beams towards CR users while nulls in the pattern are made towards PUs. This spatial CR technique allows the CR network and PUs share the same spectrum band, because the CR system can at uplink distinguish the CR signals from PUs signals by exploiting the spatial diversity technique.

Since in a CR system terminology, SUs share the spectrum of PUs, they have to limit their transmission power in order to avoid interference occurrence to PUs. This is required because the interference power received at each PU should stay below its interference temperature. However, it is noticed here that at the CR BS it is difficult to estimate accurate DOAs, when the received signals from CR users suffer from interference, noise, and multipath fading. Thus, the performance of adaptive beamformers degrades substantially due to the imperfect knowledge on the array response. On the other hand, as observed in simulations, all adaptive beamforming algorithms are limited in their ability to effectively differentiate desired signal from interferers, when DOA separation is not large enough.

Besides, all conventional adaptive algorithms are derived according to the use of uniformly polarized array elements which assumes that the polarizations of the received signals are perfectly aligned with respect to the orientation of the sensors. This assumption is rarely met in general due to the condition of the wireless propagation channel either caused by reflection, diffraction, or scattering, the signal of interest arrived at the array may contain replicas of multipath, where the two paths come in from a slightly different angle with deviated polarization and may result in polarization mismatch. This polarization mismatch will further affect the performance of adaptive beamformers.

In this thesis, we proposed to equip a CR BS receiver system with a dual-polarized array of crossed-dipole antenna in order to perform signal processing in a combined polarization-and-space domain. The proposed dual-polarized antenna array is expected to detect two orthogonal components of the impinging signals, and these two orthogonal outputs will be combined and processed by signal processing (or adaptive beamforming) techniques to minimize the effects of multipath fading and polarization mismatch loss. A dual-polarized array with adaptive beamforming algorithm has also excellent ability of cancelling broadband interferers by filtering in polarization domain in addition to DOA. This can be done by adaptively matching polarization of desired user's signal and/or nullifying interfering signals with the help of polarization orthogonallity. Hence, this can improve the link quality (or SINR) at the CR BS receiver.

It has been recognized that traditional scalar sensor arrays uses single polarization state for either transmitting or receiving the data/information thereby multiplexing based on polarization domain is unavailable. This is not an effective use of the precious spectrum resources. By using an antenna array with two orthogonally polarized array elements (e.g., horizontal and vertical), it is possible to transmit and/or receive two polarizations in azimuth by appropriately combining the two antenna outputs (to receive) or appropriately splitting the signal to be transmitted to feed the two antennas as the two channels can be used to transmit different data streams simultaneously in secondary and primary users. Thus by reusing frequencies with some combination of spatial-and-polarization division multiple accesses it is possible to improve spectral utilization.

Adaptive beamforming with dual-polarized arrays can exploit not only the DOAs of the impinging signals but also their polarizations, and can be developed either by processing the received signals in complex-valued domain or quaternion-valued domain [31-38]. Under the former case, complex-valued vectors are used to represent the output of each crossed-dipole in the array, and the collection of a crossed-dipoles array is arranged via concatenation of these vectors into a long vector. The weights of each beamformer can be obtained using either iterative algorithm or other algorithms. However, all the algorithms somehow destroy the vector nature of incident signals carrying multidimensional information in space, time, and polarization results in performance degradation.

Quaternion-valued signal processing has received more and more attentions in the recent years due to the increasing need to process three or four-dimensional signals such as; color images, vector-sensor arrays [34], three-phase power systems [35], and dual-polarization based wireless communication systems [35, 36]. Therefore, some quaternion-valued signal processing methods and algorithms have been proposed already [36-40] and due to its robustness in processing three or four-dimensional signals, a quaternion-valued signal model is chosen in this thesis. The received array output signals are first represented interms of quaternion domain. Based on the quaternion-valued steering vector model, we investigated three robust quaternion-valued adaptive beamforming algorithms, namely; Quaternion-valued Minimum Variance Distortionless Response (QMVDR) beamformer, Quaternion-valued Worst Case Constrained (QWCC) beamformer, and the well-known traditional LMS algorithm in a quaternion (QLMS) domain.

The analyses of output SINR for all algorithms are performed in two different scenarios. By analyzing the effect of sources parameters on the output SINR, the advantage is explicitly revealed that the maximum value of output SINR can be obtained either by using the orthogonallity between the polarizations of desired signal and interference or DOA difference. It is also shown in our simulation results the proposed techniques have a convincing performance improvement in terms of the output SINR level, strength of main beam, side-lobe levels, and steady state error.

This chapter is organized as follows. Section 4.2 introduces the signal and system models of two-component vector sensor arrays of crossed-dipole antenna used in CR-BS receiver system. In Section 4.3.1, 4.3.2, and 4.3.3, the proposed QMVDR, QWCC, and QLMS beamforming algorithms are discussed respectively. Finally in section 4.4 simulation results and discussions are presented.

4.2 Array and Signal Models

Due to the simple structure and lower computational complexity in practical applications, the CR-BS receiver system is assumed to be equipped with ULA of N crossed-dipole pairs as shown in Figure 4.1, where these pairs are located along the y-axis with an inter-element separation distance d, and at each location the two crossed components are parallel to the x-axis and y-axis, respectively. In each dipole pair x-axis dipole measures the horizontal polarization component of the signals and the y-axis dipole measures the vertical polarization component of the signals. Thus each dipole measures the two orthogonal signal components at a point. A dual-polarized antenna can be RHCP, LHCP, or linearly polarized.

We consider a CR user signal $s_0(t)$ as a narrowband signal with direction of arrival $\{\phi_0, \theta_0\}$ impinges upon the array among other M uncorrelated interfering signals $s_m(t),\ for\ m = 1, 2, \ldots, M$, from directions $\{\phi_m, \theta_m\}$ for $m = 1,2, \ldots, M$; where $\phi_m \in [0,2\pi)$ is the azimuth-angle, and $\theta_m \in [0, \pi)$ is the elevation-angle. Here we assume that all the incident signals have the same wavelength of λ.

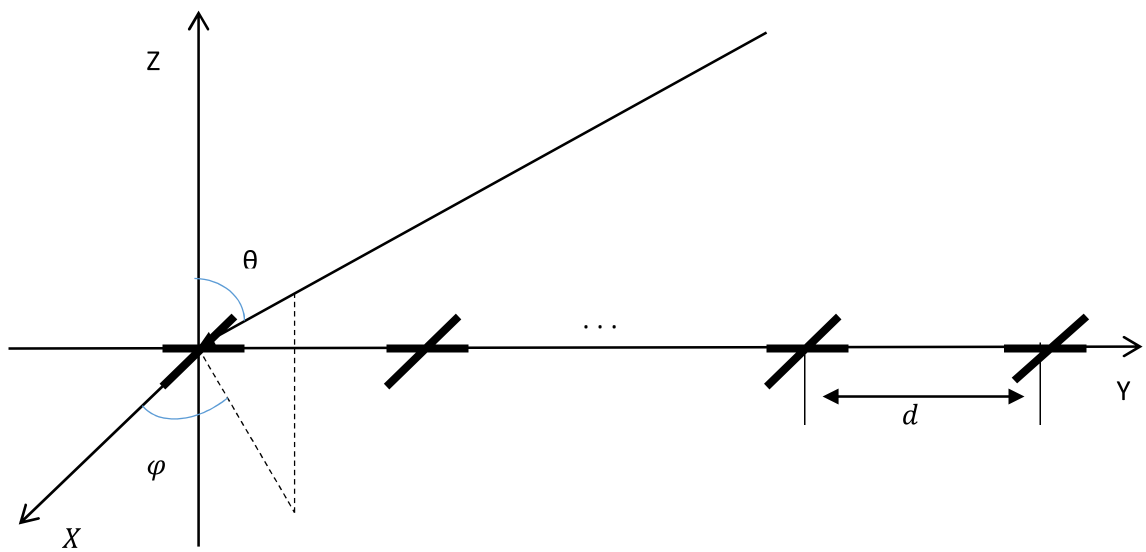

Figure 4.1 ULA of crossed-dipoles

Then, the spatial steering vector for the m^{th} signal incident on an array can be given by [35]:

$$\mathrm{a}_{s,m} = \left[1, e^{-j2\pi d \sin\theta_m \sin\phi_m/\lambda}, \ldots, e^{-j2\pi(N-1)d \sin\theta_m \sin\phi_m/\lambda}\right]^T \tag{4.1}$$

where λ is the wavelength of the incident signal and $[.]^T$ denotes the transpose operation.

Here we introduce another two interesting angles, $\gamma_m \in [0, \pi/2]$ and $\eta_m \in [0, 2\pi)$, referred to as the polarization auxiliary angle and polarization phase difference, respectively, to completely describe the polarization state of the signal. Therefore for crossed-dipoles, the spatial-polarization coherent vector of the m^{th} signal can be given by [35, 36]:

$$\mathrm{a}_{p,m} = \begin{bmatrix} -\sin\phi_m \cos\gamma_m + \cos\theta_m \cos\phi_m \sin\gamma_m\, e^{j\eta_m} \\ \cos\phi_m \cos\gamma_m + \sin\phi_m \cos\theta_m \sin\gamma_m\, e^{j\eta_m} \end{bmatrix} = \begin{bmatrix} \mathrm{a}_{p,m}^x \\ \mathrm{a}_{p,m}^y \end{bmatrix} \tag{4.2}$$

Now, we can divide the array into two sub-arrays: one is composed of all the dipoles pointing along the x-axis, while the other includes all the dipoles pointing along the y-axis. The complex valued steering vector of the x-axis sub-array for m^{th} source is given by;

$$\begin{aligned} \mathrm{a}_{x,m} &= \mathrm{a}_{s,m}.\,\mathrm{a}_{p,m}^{x} \\ &= \left(-\sin\phi_m \cos\gamma_m + \cos\theta_m \cos\phi_m \sin\gamma_m \, e^{j\eta_m}\right)\mathrm{a}_{s,m} \end{aligned} \tag{4.3}$$

and for the y-axis sub-array the complex valued steering vector is expressed as:

$$\begin{aligned} \mathrm{a}_{y,m} &= \mathrm{a}_{s,m}.\,\mathrm{a}_{p,m}^{y} \\ &= \left(\cos\phi_m \cos\gamma_m + \sin\phi_m \cos\theta_m \sin\gamma_m \, e^{j\eta_m}\right)\mathrm{a}_{s,m} \end{aligned} \tag{4.4}$$

The outputs of these two sub-arrays for all source signals can then be written as

$$x(t) = \textstyle\sum_{m=0}^{M} \mathrm{a}_{x,m} s_m(t) + n_x(t) \tag{4.5}$$

$$y(t) = \textstyle\sum_{m=0}^{M} \mathrm{a}_{y,m} s_m(t) + n_y(t) \tag{4.6}$$

where $x(t)$ and $y(t)$ represents the complex-valued outputs of horizontal and vertical components of the impinging signals respectively and $n_x(t)$ and $n_y(t) \in \mathbb{C}^{N\times 1}$ denote the corresponding additive white Gaussian noise vectors.

Now a quaternion-valued measurement vector $\boldsymbol{q}(t)$ of the crossed-dipole based linear array can be constructed in the C-expansions of quaternions, appendix-1 as follows

$$\boldsymbol{q}(t) = x(t) + iy(t) = \textstyle\sum_{m=0}^{M} \left(\mathrm{a}_{x,m} + i\mathrm{a}_{y,m}\right) s_m(t) + n_{\boldsymbol{q}}(t) \tag{4.7}$$

where $\mathrm{a}_m = \mathrm{a}_{x,m} + i\mathrm{a}_{y,m} \in \mathbb{H}^{N\times 1}$, is the quaternion-valued steering vector on two-component vector-sensor, and $n_{\boldsymbol{q}}(t) = n_{\boldsymbol{x}}(t) + in_{\boldsymbol{y}}(t)$ is the quaternion-valued noise vector consisting of the two sub-array noise vectors $n_x(t)$ and $n_y(t)$. This transformation maps the complex-valued signal $x(t)$ on scalar and j imaginary fields of a quaternion, and the complex-valued signal $y(t)$ is simultaneously mapped to the i and k imaginary fields [53].

4.3 The Proposed Adaptive Algorithms

The new system is similar to the case of single-polarization array case described in section 3.3, with the only exception of having the double amount of antenna outputs. This increases the number of available degrees of freedom. It also aids to overcome multipath channel effects and polarization mismatch loss. Furthermore it allows filtering in the polarization domain. On the other side the overall system complexity is increased, in particular the computational complexity of the matrix inversion needed for adaptive beamforming is increased. We discuss here three proposed quaternion-valued adaptive beamforming algorithms which are suitable for CR applications.

Using the quaternion-valued measurement vector $\boldsymbol{q}(n)$ in equation (4.7) of an array, the output $\boldsymbol{z}(n) \in \mathbb{H}^{N\times1}$ of a beamformer in figure 4.2 is given by,

$$\boldsymbol{z}(n) = \boldsymbol{w}^{\triangleleft}\boldsymbol{q}(n) \tag{4.8}$$

where $\boldsymbol{w} \in \mathbb{H}^{N\times1}$ is the quaternion-valued weight vector and the symbol $(.)^{\triangleleft}$ denotes the quaternion transposition-conjugation operator.

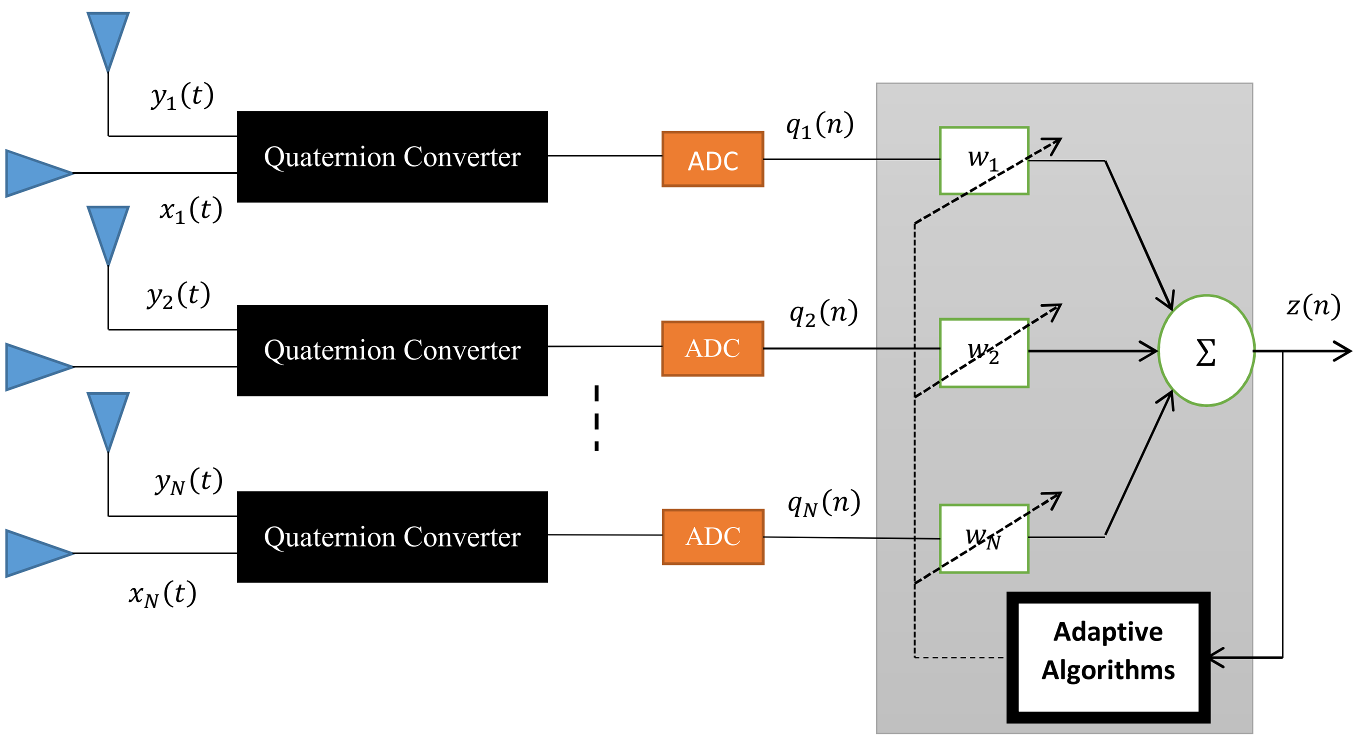

Figure 4.2 Adaptive quaternion valued algorithms.

4.3.1 Quaternion-valued MVDR Beamformer

To recover the desired signal among interferers and noise, the basic idea of Q-Capon beamforming (or QMVDR) is to keep a unity response to the desired signal at the beamformer output and then reduce the power/variance of the output as much as possible [25,32]. The key to constructing such a Q-Capon beamformer in the quaternion domain is to design an appropriate constraint to make sure the signal of interest (SOI) can pass through the beamformer with the desired unity response. Now the constraint can be formulated as

$$\boldsymbol{w}^{\triangleleft}\mathbf{a}_0 = 1 \tag{4.9}$$

where, $\boldsymbol{w}(n) = [w_1(n), w_2(n) \ \dots, w_N(n)]^T$ with $w_m(n) = a_m + ib_m + jc_m + kd_m, for\ m = 1, 2, \dots, N$ is quaternion-valued weight coefficients with $a, b, c,$ and d being real-valued, and $\mathbf{a}_0 = \mathrm{a}_{x,0} + i\mathrm{a}_{y,0}$ is the quaternion-valued steering vector of the desired signal, and $\mathrm{a}_{x,0}$ and $\mathrm{a}_{y,0}$ are the complex-valued vectors. Then, the QMVDR beamformer can be derived by solving the following constrained optimization problem:

$$J(\boldsymbol{w}) = min\{\boldsymbol{w}^{\triangleleft}R\boldsymbol{w}\}\ subject\ to\ \boldsymbol{w}^{\triangleleft}\mathbf{a}_0 = 1 \tag{4.10}$$

where, $R = E\{\boldsymbol{q}(n)\boldsymbol{q}^H(n)\}$ is the covariance matrix of the measurement vector.

Given array output data at K distinct snapshots, i.e. $\{\boldsymbol{q}(n)_{n=1}^{K}\}$, the quaternion-valued sample covariance matrix can be estimated by

$$\hat{R}(n) = \frac{1}{K}\sum_{n=1}^{K} \boldsymbol{q}(n)\boldsymbol{q}^{\triangleleft}(n) \tag{4.11}$$

Now we can apply the Lagrange multipliers methods for equation (4.10) to obtain the minimum of a function subject to the given constraint [52]. The process follows an algorithm of steps which reveal another relationship between the input variables that was neither given nor evident beforehand. We can use this relationship in conjunction with the constraint to determine critical points of the function or the vector on the constraint. First we form the Lagrange function as

$$J(\boldsymbol{w}, \lambda) = \boldsymbol{w}^{\triangleleft}R\boldsymbol{w} + \lambda\, \boldsymbol{w}^{\triangleleft}\mathbf{a}_0 \tag{4.12}$$

where λ is a quaternion-valued vector of the Lagrange multipliers.

Based on the quaternion-valued gradient operator defined in appendix A, the following gradients need to be calculated:

$$\frac{\partial J}{\partial \boldsymbol{w}^{\triangleleft}} = R\boldsymbol{w} + \lambda\mathbf{a}_0 \tag{4.13}$$

The minimum can be obtained by setting equation (4.13) equal to a zero vector [32, 33]. It is given by

$$R\boldsymbol{w} + \lambda\mathbf{a}_0 = 0 \tag{4.14}$$

Then, since $\boldsymbol{w}^{\triangleleft}\mathbf{a}_0 = -\lambda\mathbf{a}_0{}^{\triangleleft}R^{-1}\mathbf{a}_0 = 1$, we have,

$$\lambda = \frac{-1}{\mathbf{a}_0^{\triangleleft}R^{-1}\mathbf{a}_0} \tag{4.15}$$

Finally by substituting for λ from Eq. (4.15) in Eq. (4.14), the weight vector of the QMVDR beamformer can be determined as

$$\boldsymbol{w} = \frac{R^{-1}\mathbf{a}_0}{\mathbf{a}_0^{\triangleleft}R^{-1}\boldsymbol{a}_0} \tag{4.16}$$

Substituting equation (4.16) into equation (4.8), the quaternion-valued output of the QMVDR beamformer is given by

$$\boldsymbol{z}(n) = \boldsymbol{w}^{\triangleleft}\boldsymbol{q}(n) = \boldsymbol{w}^{\triangleleft}\mathrm{a}_0 s_0(n) + \sum_{m=1}^{M} \boldsymbol{w}^{\triangleleft}\left[\left(\mathrm{a}_{x,m} + i\mathrm{a}_{y,m}\right)s_m(n)\right] + w^{\triangleleft}\boldsymbol{n}_q(n) \quad (4.17)$$

where $\boldsymbol{w}^{\triangleleft}\mathbf{a}_0 = 1$ and $\boldsymbol{w}^{\triangleleft}\mathrm{a}_m \approx 0, m = 1, \dots, M$ which indicates that the interferences are nulled and the desired signal is extracted.

The SINR of quaternion-valued output $\boldsymbol{z}(n)$ can be written in the simple form as

$$SINR_0 = 10\log_{10}\frac{\boldsymbol{w}^{\triangleleft}\boldsymbol{R_d}\boldsymbol{w}}{\boldsymbol{w}^{\triangleleft}\boldsymbol{R_{i+n}}\boldsymbol{w}} \quad (4.18)$$

$$\boldsymbol{R_d} = \sigma_0^2\mathrm{a}(\vartheta_0)\mathrm{a}^{\triangleleft}(\vartheta_0), \quad (4.19)$$

$$R_{i+n} = \sum_{m=1}^{M}\sigma_{i,m}^2\mathrm{a}\left(\vartheta_{i,m}\right)\mathrm{a}^{\triangleleft}\left(\vartheta_{i,m}\right) + \sigma_n^2\mathbf{I} \quad (4.20)$$

with $\mathrm{a}(\vartheta_0)$ and $\left\{\mathrm{a}\left(\vartheta_{i,m}\right)\right\}_{m=1}^{M}$ being the steering vectors of desired signal and interferers, respectively, and σ_0^2 and $\left\{\sigma_{i,m}^2\right\}_{m=1}^{M}$ denoting their corresponding powers.

4.3.2 Quaternion Worst-Case Constrained (QWCC) Algorithm

The QMVDR beamformer is based on accurate steering vectors of incident array signals. However, steering vector mismatch usually exists in array processing as a result of DOA or polarization mismatch and various model errors. With steering vector mismatch, there will be a non-zero quaternion-valued error vector $e \in \mathbb{H}^{N\times 1}$ between assumed steering vector $\bar{\mathrm{a}}_0$ and the actual steering vector a_0, i.e.,

$$\mathrm{a}_0 = \bar{\mathrm{a}}_0 + e \quad (4.21)$$

We assume that its norm is bounded by a real positive constant ε, i.e. $\|e\| \le \varepsilon$. Then, the actual steering vector a_0 can be modeled as belonging to a steering vector set $\mathcal{A}$ defined by,

$$\mathcal{A} \triangleq \{\mathrm{a}_0 | \mathrm{a}_0 = \bar{\mathrm{a}}_0 + e, \|e\| \le \varepsilon\} \quad (4.22)$$

From equation (4.22), we can see that $\mathcal{A}$ is a spherical set where $\bar{\mathrm{a}}_0$ is in the center, and a_0 can be any vector in $\mathcal{A}$.

In order to have a robust response to the desired signal, we can impose the following constraint to the weight vector $\boldsymbol{w} \in \mathbb{H}^{N\times 1}$

$$\min_{\mathrm{a}_0\in\mathcal{A}}|\boldsymbol{w}^{\triangleleft}\mathrm{a}_0| \ge 1, \quad (4.23)$$

which is referred to as the quaternionic worst-case constraint. Under such a constraint, the magnitude of the array response for all the steering vectors in set $\mathcal{A}$ is constrained to be greater than unity.

By adopting (4.23), a robust adaptive beamformer within the quaternionic framework, named quaternion-valued worst-case constrained beamformer (QWCCB), can be formulated as follows

$$\min_{\boldsymbol{w}} \boldsymbol{w}^{\triangleleft}\hat{R}\boldsymbol{w} \quad \mathrm{s.t} \;\; \min_{\mathrm{a}_0\in\mathcal{A}}|\boldsymbol{w}^{\triangleleft}\mathrm{a}_0| \geq 1 \tag{4.24}$$

where $\widehat{\boldsymbol{R}}$ is the sample quaternionic covariance matrix in (4.11).

Equation (4.24) is reformulated; so that it can be solved by Second Order Cone (SOC) programming based method [54]. Thus, the constrained minimization problem in (4.24) can be reformulated into a convex quadratic problem as follows

$$\min_{\mathbf{w}} \boldsymbol{w}^{\triangleleft}\hat{R}\boldsymbol{w} \;\; \mathrm{s.t} \;\; \begin{array}{c} \mathrm{Re}\{\boldsymbol{w}^{\triangleleft}\bar{\mathrm{a}}_0\} \geq 1+\varepsilon\|\mathbf{w}\| \\ \mathrm{Im}^{(i)}\{\boldsymbol{w}^{\triangleleft}\bar{\mathrm{a}}_0\} = 0 \\ \mathrm{Im}^{(j)}\{\boldsymbol{w}^{\triangleleft}\bar{\mathrm{a}}_0\} = 0 \\ \mathrm{Im}^{(k)}\{\boldsymbol{w}^{\triangleleft}\bar{\mathrm{a}}_0\} = 0 \end{array} \tag{4.25}$$

4.3.3 Quaternion Least Mean Squares (QLMS) Algorithm

The QLMS adaptive beamforming algorithm is similar to the convention scalar sensor based LMS algorithm, but the only difference is it uses the quaternion-valued measurement signal $\boldsymbol{q}(n)$ and the corresponding quaternion-valued weight $\boldsymbol{w}$. With available quaternion-valued reference signal $d(n)$ and the beamformer output $z(n)$, LMS adaptive beamforming algorithm can be derived in quaternion domain.

The error signal $e(n)$ is generated by the difference between the reference signal and the beamformer output, which is given by

$$e(n) = d(n) - \boldsymbol{w}^T\boldsymbol{q}(n) \tag{4.26}$$

where

$$\boldsymbol{w}(n) = [w_1(n), w_2(n) \;\; \dots, w_N(n)]^T \tag{4.27}$$

$$\boldsymbol{q}(n) = [q_1(n), q_2(n), \dots, q_N(n)]^T \tag{4.28}$$

The conjugate form of the error signal is $e^*[n]$, given by

$$e^*(n) = d^*(n) - \boldsymbol{q}^H(n)\boldsymbol{w}^* \tag{4.29}$$

where $\{.\}^H$ is the combination of both $\{.\}^T$ and $\{.\}^*$ operations for a quaternion. Then $\boldsymbol{w}$ can be updated by minimizing the instantaneous square error.

The cost function $J(n)$ is constructed by using the MSE [19, 20] and can be expressed as

$$J(n) = e(n)e^*(n)$$
$$= d(n)d^*(n) - d(n)\boldsymbol{q}^H(n)\boldsymbol{w}^*(n) - \boldsymbol{w}^T(n)\boldsymbol{q}(n)d^*(n) + \boldsymbol{w}^T(n)\boldsymbol{q}(n)\boldsymbol{q}^H(n)\boldsymbol{w}^*(n) \quad (4.30)$$

As discussed in [20], the gradient of $J(n)$ with respect to $\boldsymbol{w}^*$ would give the steepest direction for the optimization surface. Details of the derivation process for the gradient is presented in [31, 32] and obtained as follows

$$\nabla_{\boldsymbol{w}^*} J(n) = -\frac{1}{2} e(n)\boldsymbol{q}^*(n) \quad (4.31)$$

Finally, the update equation of QLMS-based adaptive algorithm with step size μ is expressed as

$$\boldsymbol{w}(n+1) = \boldsymbol{w}(n) - \mu \nabla_{\boldsymbol{w}^*} J(n) \quad (4.32)$$

Substituting equation (4.35) into equation (4.36) leads to the following QLMS algorithm

$$\boldsymbol{w}(n+1) = \boldsymbol{w}(n) + \frac{1}{2}\mu\{e(n)\boldsymbol{q}^*(n)\} \quad (4.33)$$

Using the above adaptive QLMS algorithm, we can find the optimal coefficient vector in terms of minimum mean square error (MSE) and obtain a satisfactory beamforming result.

4.4 Simulation Results and Discussion

In this section, the proposed quaternion-valued adaptive beamforming algorithms which are described in section 4.3 are programmed in MATLAB and simulations are carried-out to obtain their performances. The comparison of the algorithms will focus on output SINR and resultant beampattern performance of different algorithms. These performance surfaces for the proposed QMVDR, QWCC, and QLMS beamformers are tested in two different scenarios. In the first scenario we consider the condition for which desired and interfering signals having identical polarization states, but with different DOA separations. This baseline scenario has the aim to verify if the additional polarization channel improves signal reception, i.e. in terms of out-SINR.

In the second scenario, we test the condition for which the desired signal and interferers having fixed DOA separation, but with various polarizations state separation or polarization parameters. The objective of the second test scenario is to show the capability of the proposed algorithms in interference mitigation by polarization degree. In these simulations the effect of signal polarization information on beamformers performance are clearly revealed. Finally the performances of our quaternion-valued algorithms are compared with conventional scalar array based adaptive algorithms which is presented in chapter three.

4.4.1 Description of System Parameters

We assume a CR BS receiver system equipped with a ULA of 10 crossed-dipoles spaced half a wavelength $(\mathrm{d} = \lambda/2)$ apart. We consider three users; one CR user along with two uncorrelated interfering signals are impinging upon the array, and that the steering vectors of CR user signal and interferers (i.e., DOA and polarization parameters) will be estimated by some techniques and assumed accurately known as prior information. The binary phase shift keying (BPSK) modulation is used and the background noise is zero-mean quaternion-valued Gaussian. The SNR of CR user signal is $10\ dB$ and each of interference signal has interference-to-noise ratio (INR) of $20\ dB$. For each scenario, 200 independent runs are used to calculate each simulated value.

4.4.2 Scenario 1: Performance with Different DOA Separations

In this case, we study the resultant beampattern and output-SINR performance, where the desired signal and interferers having identical polarization states, but with different DOA separations. First, we give the beampatterns of the proposed beamformers to verify their effectiveness in case of small angle separation. For convenience we assumed that all signals arriving from the same plane of $\phi = 90^0$. The CR user signal is assumed to arrive from elevation angle of $\theta_d = 0^0$, and three different DOAs of interferers are considered and provided in table 4.1 below. All signals have the same polarization parameters of $(\gamma, \eta) = (45^0, 0^0)$. Three proposed approaches QMVDR, QWCC, and QLMS beamformers are compared using the same type of array in terms of beam pattern and averaged output SINR.

Table 4.1 DOAs of Interferers

Users	DOAs in elevation angle		
Interferer 1 (θ_{i1})	-10^0	-30^0	-45^0
Interferer 2 (θ_{i2})	10^0	30^0	45^0

Figure 4.3 displays the resultant beampatterns of QMVDR for various DOA separation between desired signal and interferences for the fixed $SNR = 10\ dB$. From this figure one can observe that for large angular separation, QMVDR produces maximum radiation to desired direction at 0^0, while interfering signals have all been effectively suppressed, and sidelobe levels are also minimum. Although, our proposed QMVDR algorithm for small angle separation do not have

nulls at the DOAs of the interferences as deep as that of large angle separation, the interferences are sufficiently suppressed and it can still places maximum radiation to desired direction. Hence QMVDR has better performance compared to conventional adaptive beamformers, and this performance improvement is due to additional information provided from orthogonal component.

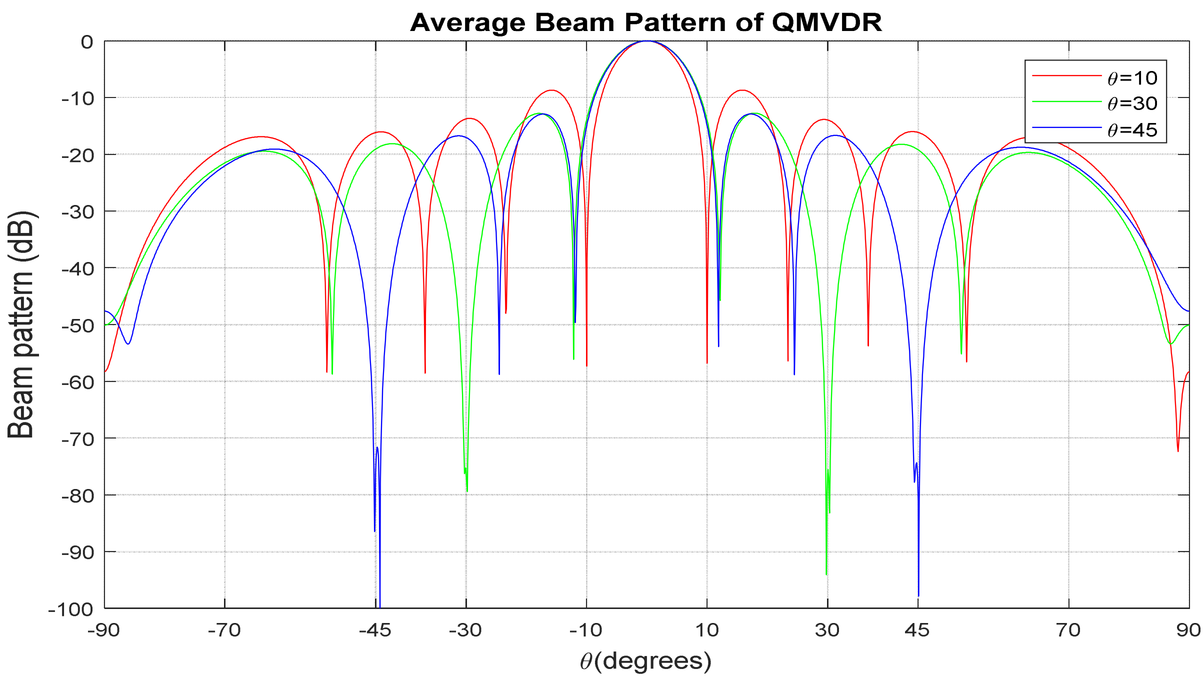

Figure 4.3 Beam pattern of QMVDR for: $N = 10$, $SNR = 10\ dB$, $INR = 20\ dB$, $\theta_d = 0^0$, and $(\gamma, \eta) = (45^0, 0^0)$.

Figure 4.4 shows the resultant beampattern plot of QWCC beamformer for similar parameters considered with various DOA separations. From this figure one can observe that for large angle separation, QWCC produces maximum radiation to desired direction at 0^0 and place deep nulls in the direction of interfering signals as QMVDR. The QWCC beamformer has almost similar performance characteristics for small and large angle separation. One of the interesting characteristics of QWCC is its robustness to DOA uncertainties. Thus in the case of small angle separation and DOA uncertainties QWCC has better performance than QMVDR. In addition, it should also be emphasized that performance of conventional adaptive algorithms for DOA uncertainty is not mentioned in this paper, their performance further becomes worse when steering vector mismatch exists.

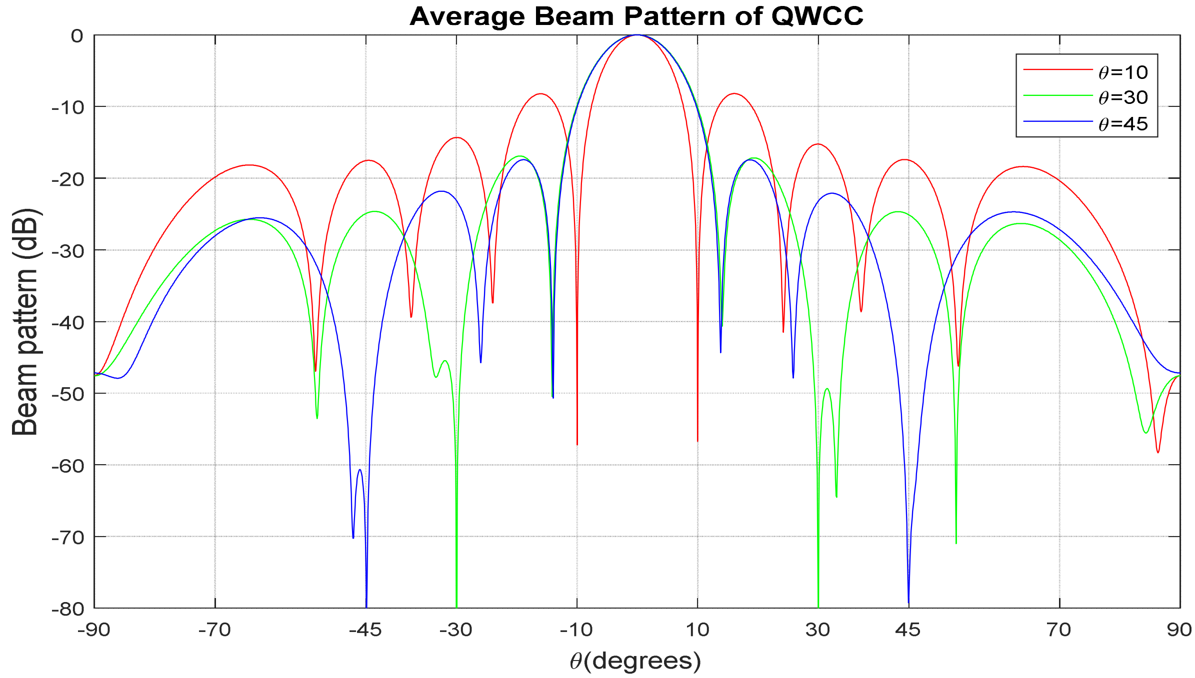

Figure 4.4 Beampattern of QWCC for; $SNR = 10\ dB, INR = 20\ dB, \theta_d = 0^0$, and $(\gamma, \eta) = (45^0, 0^0)$.

The 2-D beampattern for the third proposed QLMS algorithm is provided in Figure 4.5. We can see from QLMS simulation result that the interferences from their known DOAs have been all suppressed deeply even when they are close to desired user. This shows QLMS algorithm has better interference cancellation capability than either QMVDR or QWCC beamformer. Moreover, a large magnitude response is formed around the direction of the desired signal.

Figure 4.6 is plotted to compare the main beamwidth, nulling capability, and side lobe levels of all proposed algorithms by assuming the same polarization parameters with sufficient angle separation between CR user signal and interferers. According to the simulation results all algorithms produced maximum beampattern to desired direction and effectively formed two nulls towards -30^0 and 30^0. The main beamwidth of QMVDR beamformer is narrow compared to QWCC and QLMS beamformers. The QWCC and QLMS algorithms have the lowest side lobe levels while QMVDR algorithm has the highest side lobe level.

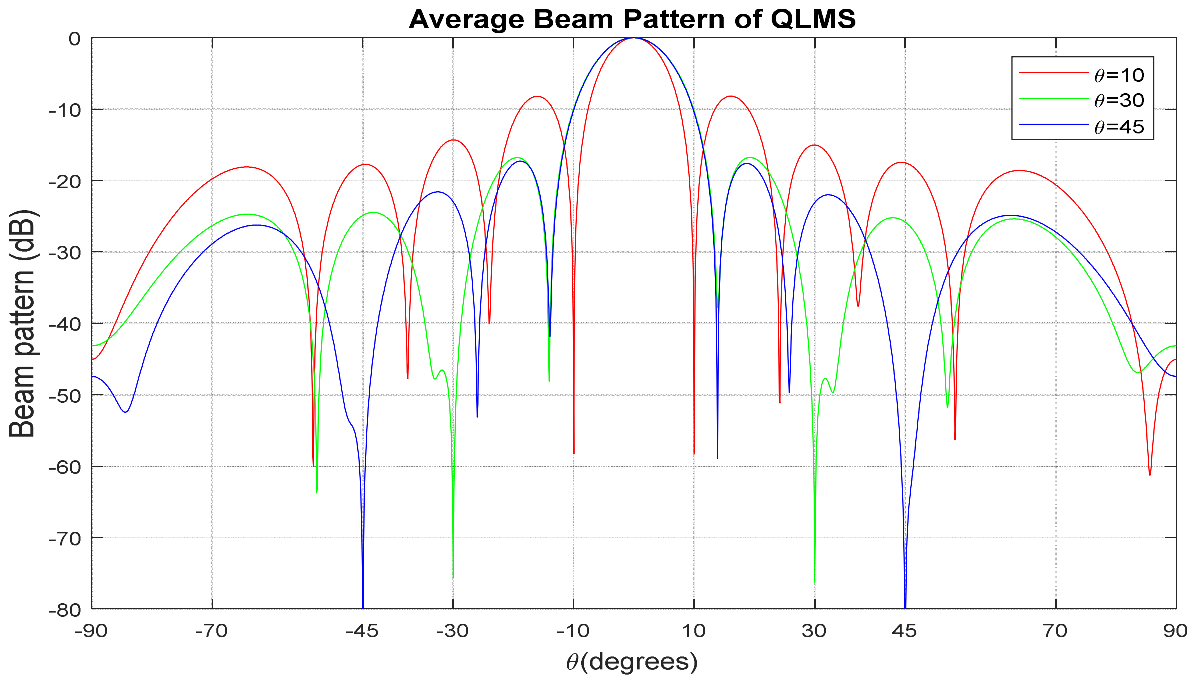

Figure 4.5 Beampattern of QLMS for: $SNR = 10\ dB, INR = 20\ dB$, $\theta_d = 0^0$, and $(\gamma, \eta) = (45^0, 0^0)$.

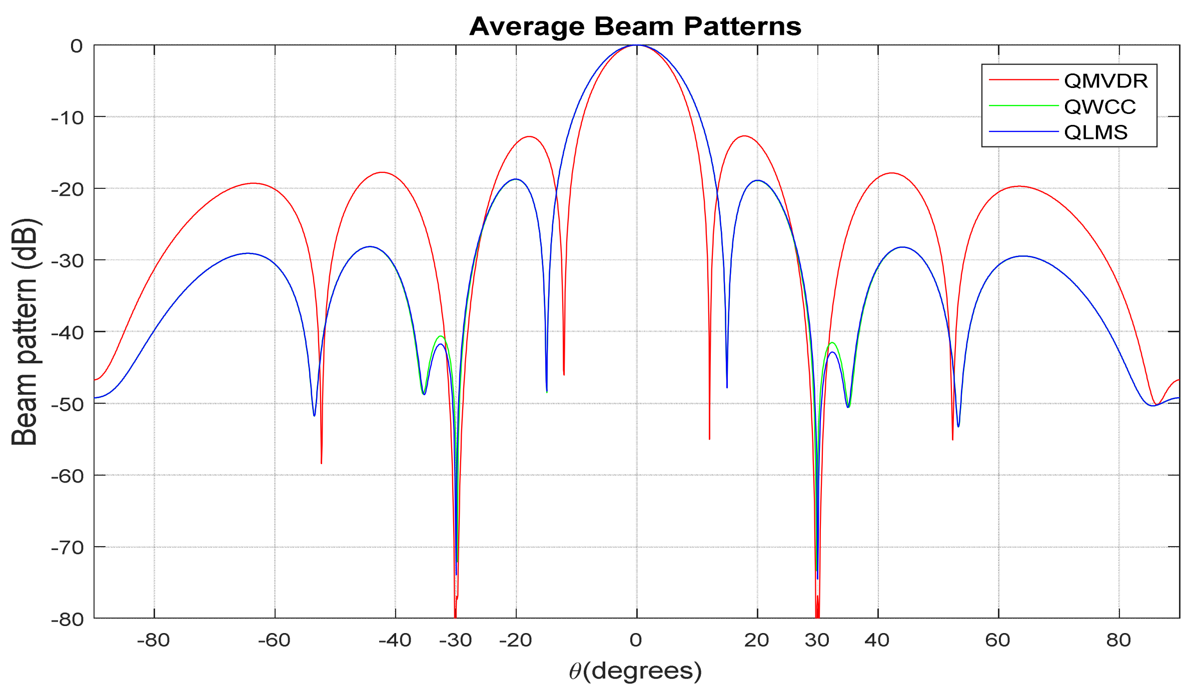

Figure 4.6 Beam patterns of all proposed algorithms for; $N = 10$, $SNR = 10\ dB$, $INR = 20\ dB$, $\theta_d = 0^0$, and two interferences are from -30^0 and 30^0.

Figure 4.7 shows the output SINR performance versus input SNR of the proposed QMVDR, QWCC, and QLMS beamformers with 1000 snapshots. It can be seen that for most of the input SNR range, the QWCC and QLMS beamformers have the best output SINR performance versus the input SNR, while the QMVDR performance slightly drops at upper ranges, but it still outperforms the conventional beamformers. In the lower SNR range, all beamformers have a similar result, but the gap becomes greater from input $SNR = 10\ dB$ onwards.

Table 4.2 Tabulation of output $SINR$ versus input SNR for scenario one

Types of Beamformer	SNR(dB)										
	-20	-15	-10	-5	0	5	10	15	20	25	30
QMVDR	-10.49	-5.55	-0.5	4.47	9.23	14.36	18.11	19.28	19.69	20.52	26.21
QWCC	-10.49	-5.49	-0.5	4.46	9.24	14.37	19.24	24.35	29.39	34.25	39.34
QLMS	-10.48	-5.49	-0.52	4.41	9.20	13.82	18.40	23.14	28.03	32.99	37.98

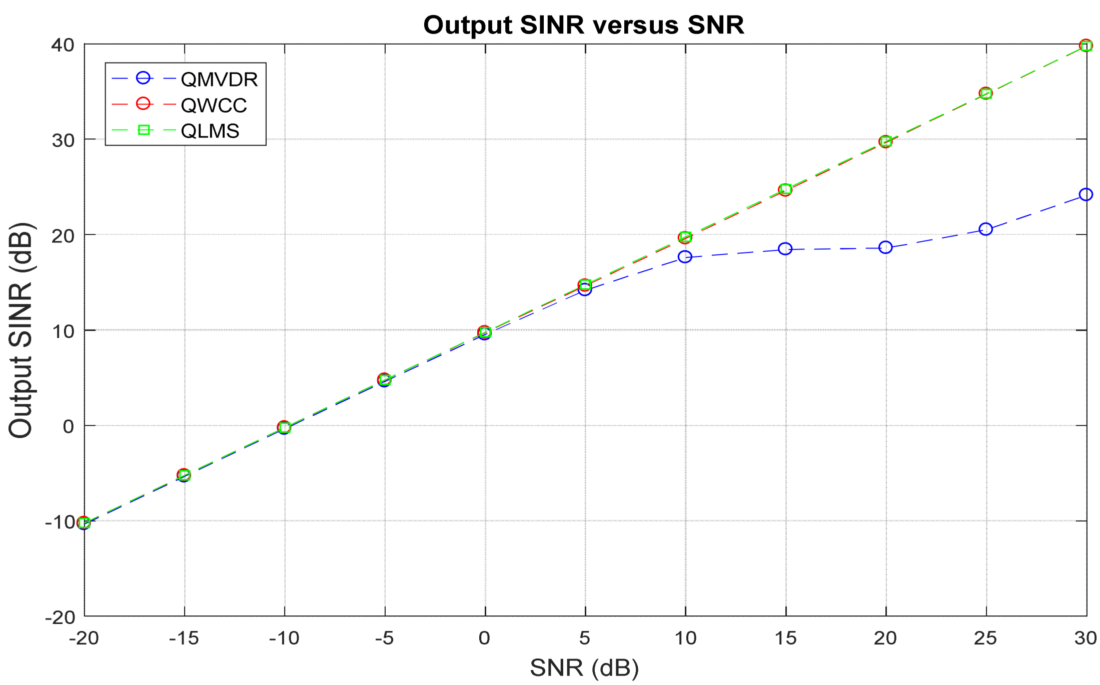

Figure 4.7 Output SINR vs input SNR: $SNR = -20\ up\ to\ 30\ dB$, $INR = 10\ dB$, $\theta_d = 0^0$, $\theta_{i1} = -30^0$, $\theta_{i2} = 30^0$ and $(\gamma, \eta) = (45^0, 0^0)$.

The output SINR with respect to the number of snapshots for fixed SNR is shown in figure 4.8.

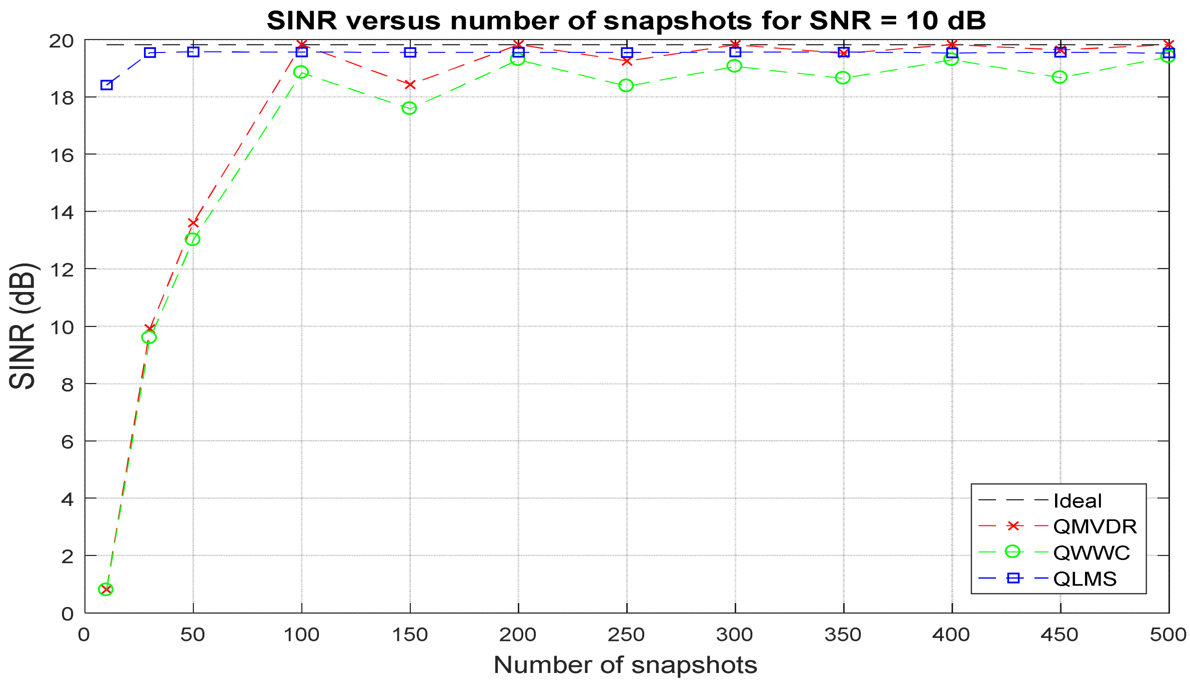

Figure 4.8 Output-SINR versus number of snapshots for; $N = 10$, $INR = 20\ dB$, $\theta_d = 0^0$, $\theta_{i1} = -30^0$ and $\theta_{i2} = 30^0$.

4.4.3 Scenario 2: Performance with Various Polarization Differences

For this case, we investigate a condition for which the desired signal and interferers having fixed DOA separation, but with various polarization deviation between signals. In this scenario polarization differences of signals may be further classified into two different conditions. The first case is the desired and interfering signals having identical polarization states (e.g. linear polarization, RHCP, and LHCP) with deviated orientation. The second condition is signals having different polarization states, for instance circularly polarized desire user signal and linearly polarized interfering signals. Nevertheless we consider here the general case of arbitrary polarized desired and interfering signals.

For convenience, we assume all signals arriving from the same plane as in the previous case, i.e., $\phi = 90^0$. The CR user signal is assumed to arrive from elevation angle of $\theta_d = 0^0$, and the two interferers' arrive from fixed elevation angles of -30^0, and 30^0. The various polarization parameters of CR user and interfering signals are provided in table 4.3

Table 4.3 Polarization Parameters

Users	DOA (ϕ, θ)	Polarizations (γ, η)		
CR user	$(90^0, 0^0)$	$(60^0, 60^0)$	$(45^0, 90^0)$	$(15^0, 50^0)$
Interferer one	$(90^0, 30^0)$	$(60^0, 75^0)$	$(60^0, 90^0)$	$(35^0, 80^0)$
Interferer two	$(90^0, -30^0)$	$(60^0, 75^0)$	$(60^0, 90^0)$	$(85^0, 110^0)$

Figures 4.9, 4.10, and 4.11 are plotted to study the beampattern performances of QMVDR, QWCC, and QLMS beamformers, by assuming elliptically polarized desired and interfering signals with identical ellipticities but different tilt angles. It is seen that all three beamformers steer almost a zero towards the interferences' DOA (located at -30^0 and 30^0) in all cases. One thing we can visualize from these plots is that when there is a polarization difference between desired signal and interferences all algorithms place deep nulls in interfering direction. This is because of algorithms capability in filtering both in DOA and polarization differences. If overall performance is considered QWCC and QLMS out performs QMVDR.

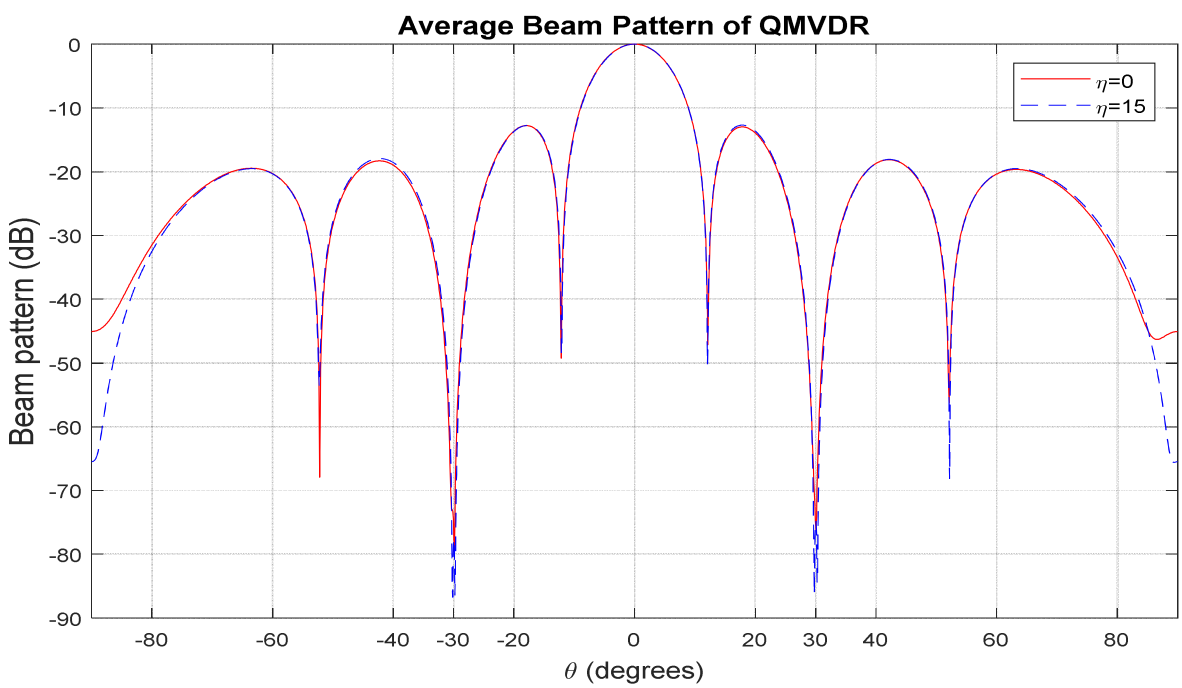

Figure 4.9 Beam pattern of QMVDR for; $N = 10$, $SNR = 10\ dB$, $INR = 20\ dB$, $(\theta_d, \gamma_d) = (0^0, 60^0)$, $(\theta_{i1}, \gamma_{i1}) = (-30^0, 60^0)$, and $(\theta_{i2}, \gamma_{i2}) = (30^0, 60^0)$.

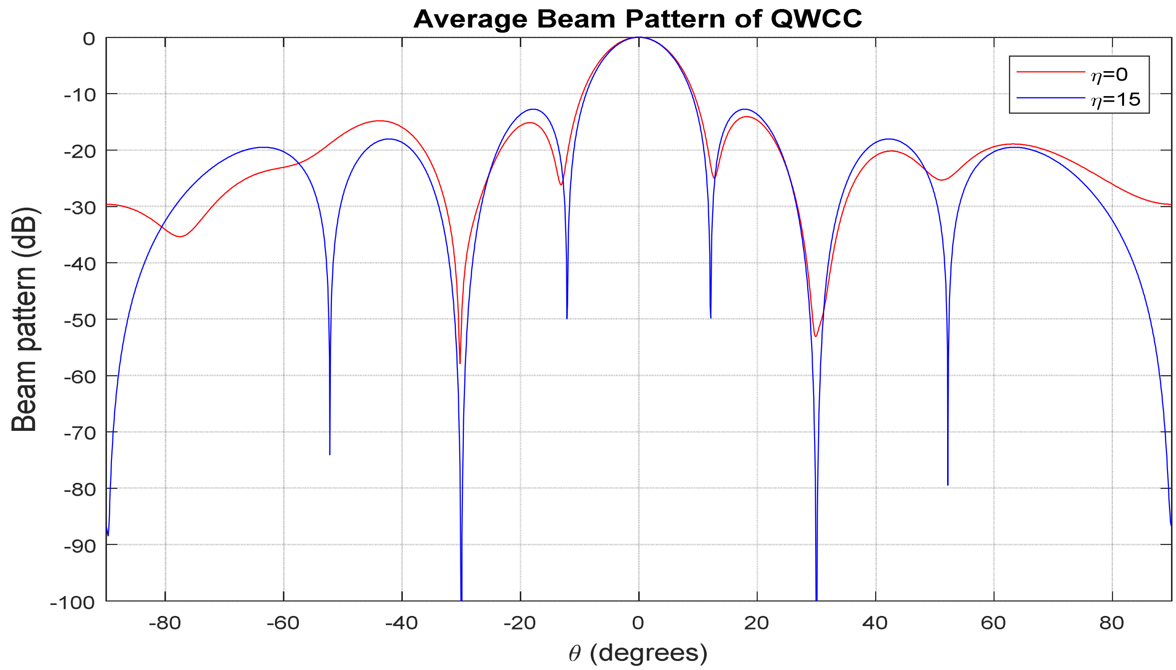

Figure 4.10 Beam patterns of QWCC for; $N = 10$, $SNR = 10\ dB$, $INR = 20\ dB$, $(\theta_d, \gamma_d) = (0^0, 60^0)$, $(\theta_{i1}, \gamma_{i1}) = (-30^0, 60^0)$, and $(\theta_{i2}, \gamma_{i2}) = (30^0, 60^0)$.

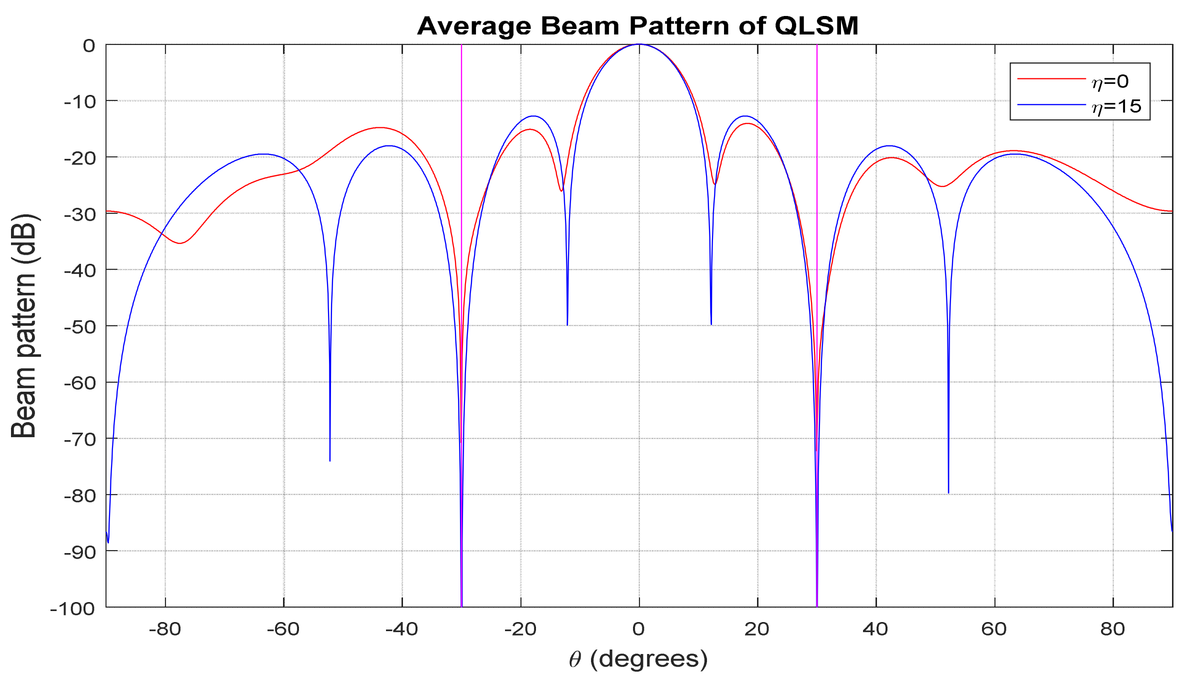

Figure 4.11 Beam patterns of QLMS for; $N = 10$, $SNR = 10\ dB$, $INR = 20\ dB$, $(\theta_d, \gamma_d) = (0^0, 60^0)$, $(\theta_{i1}, \gamma_{i1}) = (-30^0, 60^0)$, and $(\theta_{i2}, \gamma_{i2}) = (30^0, 60^0)$.

From figure 4.12, it is again observed that the QLMS beamformer is still the overall best performer among the three beamformers. As for the second best performing beamformer, it is a tie between the QMVDR beamformer (at low to moderate SNR) and the QWCC robust beamformer (at highest SNR). An illustration of the output $SINR$ results for all the beamformers shown in Figure 4.12 is as shown in table 5.4 below:

Table 4.4 Tabulation of $SINR_0$ versus SNR for Scenario two

Types of Beamformer	SNR(dB)										
	-20	-15	-10	-5	0	5	10	15	20	25	30
QMVDR	-10.49	-5.55	-0.5	4.47	9.23	14.36	19.11	24.28	27.69	33.49	33.91
QWCC	-10.49	-5.49	-0.5	4.46	9.24	14.37	18.40	23.14	28.39	34.25	39.34
QLMS	-10.48	-5.49	-0.52	4.41	9.20	13.82	19.24	24.35	29.39	34.99	39.98

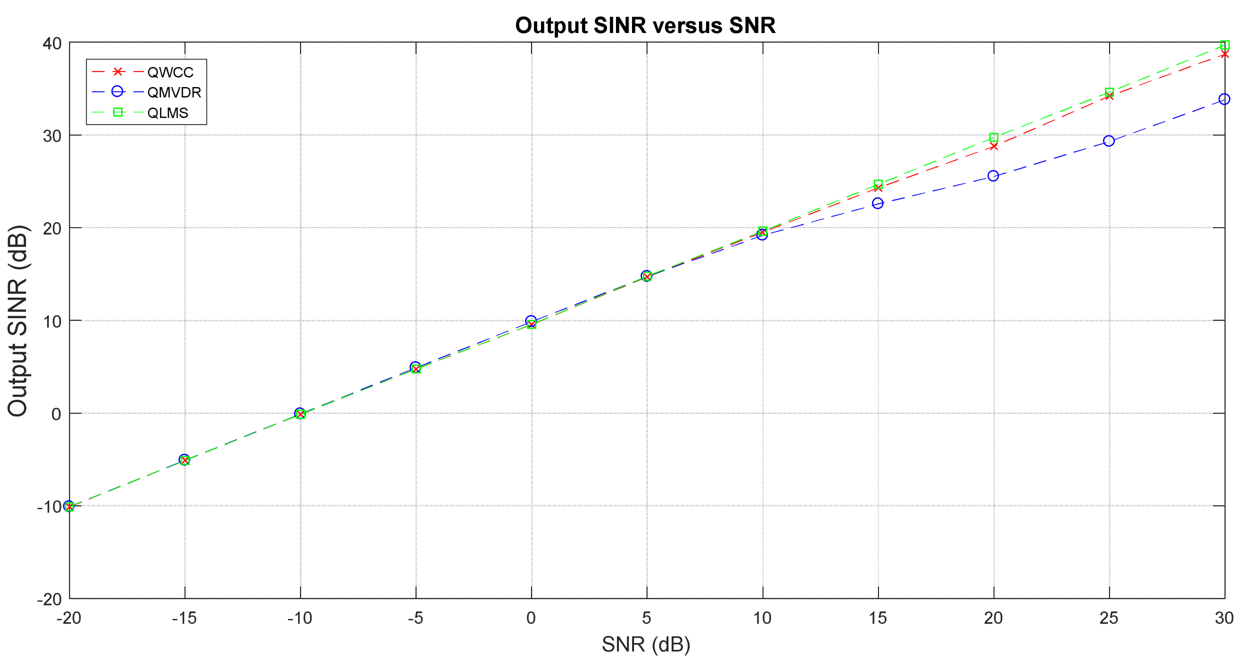

Figure 4.12 SINR versus SNR for; $N = 10$, $(\theta_d, \gamma_d) = (0^0, 45^0)$, $(\theta_{i1}, \gamma_{i1}) = (-20^0, 60^0)$, and $(\theta_{i2}, \gamma_{i2}) = (20^0, 60^0)$.

CHAPTER FIVE

CONCLUSION AND FUTURE WORK

5.1 Conclusion

In comparison to the existing wireless communication concept which virtually deploys fixed spectrum band for different wireless technologies, the concept of CR technology is indicative in bringing the wireless technology to new era. One of the CR objectives is to obtain efficient spectrum utilization. We have proposed an integrating dual polarized antenna array with beamforming technique into the CR receiver system, which fully exploits spatial and polarization diversity and thus greatly leverages polarization/spatial cognition capability to achieve a most efficient spectrum utilization and full spectrum sharing with PUs. The main concerns about applying combined polarization-and-space signal processing techniques to CR-BS system is to be able to detect CR user signals in the presence of PUs interference at CR receiving.

At the CR-BS system, the main challenge is to detect and receive signals from CR users, when CR user SNR is low in the presence of PUs interference. Conventional adaptive beamforming algorithms were proposed for CR-BS application to improve SINR of desired signal and mitigate interferences. However the performances of conventional adaptive beamformers degrades in cases of low SNR, polarization mismatch, and small DOA separation as seen in part one simulation, and applying them to CR-BS is limited in these cases.

We therefore proposed to equip a CR-BS receiver system with dual-polarized antenna array. In the beamformer design three robust quaternion signal model based adaptive algorithms QMVDR, QWCC, and QLMS are investigated for the uplink application of CR BS system. We provided a detailed discussion and mathematical analysis of these algorithms and created a MATLAB simulation to compare their performance with that of algorithms presented in chapter three. The resultant beampattern and output-SINR performances of all these algorithms are compared under different test conditions (e.g., various signal polarization, different DOA, and input SNR. It was also shown from the simulation results that all proposed algorithms, QMVDR, QWCC and QLMS, can outperform the conventional beamformers in all the test conditions). If overall performance is considered QLMS beamformer has better performance and preferred for CR-BS application. Finally, we also provide a detailed survey of the conventional adaptive beamforming algorithms, which is very useful for the researchers working in this area.

5.2 Future Work

Although we have investigated the optimal antenna array with adaptive beamforming for various DOA separation and polarization parameters based on different performance criteria's, which are presented in this work are useful for CR system, there are still some issues that require further research for further improvement. Below are lists of some recommendations for further extension of this thesis work.

- In this thesis, the performance of all the algorithms is evaluated by using a uniform linear array of crossed-dipoles. In the future, we can use different array geometries, e. g., circular array, planar, and conformal array.
- The coupling effect in this work is not considered. Thus the work can be extended by including coupling effect.
- In this work the steering vector information is considered to be accurately known, the work can be extended to include array steering vector errors.
- In this research, we only use a simple channel model to evaluate the performance of the algorithms. It may be useful if a channel model including the DOA, the time delay, the power level, and the time-varying property of each multipath can be used in the simulation.
- In this work, when the angle difference is 0 degree, it is very challenging to differentiate the desire and the interferer signal. Thus, the work can be extended to alleviate such type of problem either by modify the available algorithm or introduce the new one.

Appendix A

Quaternion Algebra

Quaternion was introduced by W. R. Hamilton [21]. It is obvious that the quaternion signal model is more suitable for two component vector sensor array signal processing than the conventional long vector signal model which is based on the complex number. A quaternion $q \in \mathbb{H}^1$ is constructed by four components, with one real part and three imaginary parts, defined as

$$q = q_1 + (q_2 i + q_3 j + q_4 k), \quad \text{(A.1)}$$

Where $q_1, q_2, q_3,$ and q_4 are real-valued. The three imaginary units $i, j, and\ k$ satisfy

$$ij = k,\ jk = i,\ ki = j$$
$$ijk = i^2 = j^2 = k^2 = -1 \quad \text{(A.2)}$$

The conjugate of a quaternion, denoted by q^*, is given by

$$q^* = q_1 - q_2 i - q_3 j - q_4 k \quad \text{(A.3)}$$

A quaternion number $q = q_1 + (q_2 i + q_3 j + q_4 k)$ can be conveniently expressed as a combination of two complex numbers c_1 and $c_2 \in \mathbb{C}$ as follows

$$q = c_1 + i c_2 = (q_1 + j q_3) + i(q_2 + j q_4) = q_1 + q_2 i + q_3 j + q_4 k \quad \text{(A.4)}$$

A.1 Quaternion Vector and Matrix

Quaternion vectors and matrices are quite different from real and complex ones. For quaternion vectors, the space can be denoted by two different bases left-spanned and right-spanned given by

$$span_L\{u_1, u_2, \dots, u_M\}, span_R\{u_1, u_2, \dots, u_M\}. \quad \text{(A.5)}$$

Here we use q_L to denote the left linear combination case and q_R to denote the right linear combination case. Note that $q\ = q_L = q_R$,

$$q_L = \sum_{m=1}^{M} \tau_m u_m \quad \text{(A.6)}$$

$$q_R = \sum_{m=1}^{M} \gamma_m u_m \quad \text{(A.7)}$$

where $\tau_m, \gamma_m \in \mathbb{H}, for\ m = 1, 2, \dots, M$.

Similarly, the Eigen decomposition operation for quaternion matrices also differs from real and complex ones. We can also define the left Eigen-decomposition Q_L and right Eigen decomposition Q_R

For a Hermitian matrix $Q \in \mathbb{H}^{N\times N}$, $(Q = Q^H$, where $\{\}^H$ is the Hermitian transpose, a combination of quaternion-valued conjugate and transpose operations.

$$\begin{aligned} Q_L &= \textstyle\sum_{n=1}^{N} \alpha_n u_n u_n^H \\ Q_R &= \textstyle\sum_{n=1}^{N} u_n u_n^H \beta_n \end{aligned} \tag{A.8}$$

where α and β are the left and right eigenvalues [32,33].

A.2 Gradient for a Quaternion function

Let $l(\boldsymbol{w})$ be a scalar function of the quaternion-valued vector $\boldsymbol{w} \in \mathbb{H}^{N\times 1}$, with $\boldsymbol{w} = [w_1 \dots w_n \dots w_N]^T$, and $w_n = a_n + ib_n + jc_n + kd_n$.

Its gradient with respect to $\boldsymbol{w}$ is defined by

$$\nabla_w l = \left[\nabla_{w_1} l \ \dots \ \nabla_{w_n} l \ \dots \ \nabla_{w_N} l\right]^T \tag{A.9}$$

Where,

$$\nabla_{w_n} l = \frac{1}{4}\left(\nabla_{w_{na}} l + \nabla_{w_{nb}} li + \nabla_{w_{nc}} lj + \nabla_{w_{nd}} lk\right) \tag{A.10}$$

$$\nabla_{w_n^*} l = \frac{1}{4}\left(\nabla_{w_{na}} l - \nabla_{w_{nb}} li - \nabla_{w_{nc}} lj - \nabla_{w_{nd}} lk\right) \tag{A.11}$$